ASSESSMENT OF OIL AND GAS RESOURCES IN THE VACA MUERTA SHALE, NEUQUÉN BASIN, ARGENTINA

A Thesis

by

JUAN CRUZ MAYOL

Submitted to the Office of Graduate and Professional Studies of
Texas A&M University
in partial fulfillment of the requirements of the degree of

MASTER OF SCIENCE

Chair of Committee, Duane McVay
Co-chair of Committee, John Lee
Committee Members, Thomas A. Blasingame
Ruud Weijermars
Head of Department, Jeff Spath

May 2019

Major Subject: Petroleum Engineering

ABSTRACT

According to the 2015 Energy Information Administration (EIA) global assessment (EIA 2015), Argentina ranks third among countries in shale-gas resources and fourth in shale-oil resources. The Vaca Muerta formation in the Neuquén basin holds most of these resources. After the first EIA assessment of these resources in 2011, there has been a huge increase in investment, given the interest of the Argentine government to recover the energy autonomy it lost in the 1990s. The rush to start production led to the drilling of vertical wells designed to take advantage of the thickness of the formation, of up to 500 m (1640 ft). The poor results of the vertical wells made some investors reconsider the potential of the Vaca Muerta formation. In 2014, YPF drilled the first horizontal wells in cooperation with Chevron. The good results of these horizontal wells attracted more operators to invest in Vaca Muerta, either independently or through joint ventures with YPF. Four years later, with more production data available, it is possible to re-evaluate the potential volumes of oil and gas that are technically recoverable.

Accurate estimation of the resource size and future production, as well as the uncertainties associated with them, is critical for making development decision for these shale oil and gas resources. A probabilistic-decline-curve-analysis method was chosen to incorporate the publicly available data production data into play-wide study in a simple and fast way, as well as to quantify uncertainty.

The Vaca Muerta formation was subdivided into sub-areas based on the fluid type. The most appropriate decline model was determined for each sub-area and coupled with Markov-Chain-Monte-Carlo (MCMC) methodology to analyze and forecast production of existing wells to calculate reserves. The analyses of individual wells in each sub-area were used to

create probabilistic type-decline curves. These curves were combined with the estimated acreage per well distributions and the remaining drillable areas per sub-area to estimate contingent and prospective resources. The difference between contingent and prospective resources was based on the distance from existing wells.

As of January 2018, the total reserves (P90–P50–P10) for the Vaca Muerta shale in Argentina associated with existing wells are estimated to be 8.5–17.5–38.4 MMm^3 of oil and 9.5–27.2–74.6 Bm^3 of gas. Estimated contingent resources are 8.8–50.6–181.1 MMm^3 of oil and 2.6–16.4–51.5 Bm^3 of gas. Estimated prospective resources are 424–2,464–8,771 MMm^3 of oil and 211–1,279–3,483 Bm^3 of gas. Resources and reserves were combined to estimate the technically recoverable resources (TRR). The estimated TRR were 443–2533–8992 MMm^3 of oil and 223–1223–3609 Bm^3 of gas.

The P10/P90 ratio of the oil TRR estimate, 21.27, is a more realistic estimate of the actual uncertainty compared to the 2.02 ratio of the only other probabilistic study by Gutierrez Schmidt et al. (2014). The other, deterministic, oil estimates of previous studies fall within the range of the estimates provided in this thesis. The gas estimates of this thesis are significantly lower than those in previous deterministic volumetric estimates, but slightly higher than the P10 estimate from YPF (2011).

This is the first public estimate conducted using production data from existing wells. The results of this work should provide a more reliable assessment of the size and uncertainties of the resources in the Argentine Vaca Muerta shale than previous estimates obtained through volumetric methodologies and analogies.

DEDICATION

This thesis is dedicated to my grandfather.

CONTRIBUTORS AND FUNDING SOURCES

This work was supervised by a thesis committee consisting of Professor McVay, my advisor, Professor Lee, my co-chair, and Professor Weijermars of the Department of Petroleum Engineering, Professor Blasingame of the Department of Geology.

The software used for the simulations was developed and provided by Dr Gong, Dr Gonzalez, and Dr McVay.

All work for the thesis was completed independently by the student.

There are no outside funding contributions to acknowledge related to the research and compilation of this document.

TABLE OF CONTENTS

Page

LIST OF FIGURES

Page

LIST OF TABLES

Page

1. INTRODUCTION

1.1. Global context and problem statement

The success of unconventional oil and gas in North America led to an increase in interest in other shale plays around the world. Argentina's Vaca Muerta shale in the Neuquén basin was no exception. Its world-class properties led the Argentine government to see in this black shale the possible solution to the country's energy crisis. Because of Vaca Muerta's outstanding properties, as well as incentives from the government to satisfy the country's energy needs (Ministerio de Energia y Mineria de la Republica Argentina 2016), investors seemed to be determined to produce the source rock. Even after the downturn of oil and gas prices beginning in 2014, there has been an investment of $10 billion dollars by 2018 based on signed agreements, according to the Argentine Energy Minister (Argentina Shale 2017). The positive results seen by the pioneer projects attracted more companies to invest to produce from the Vaca Muerta formation: Shell, Dow Chemicals, Petronas, Wintershall, XTO, Equinor, Pampa Energia, Pluspetrol, Tecpetrol, and Total. Although there are several identified shale plays in Argentina, Vaca Muerta has the highest expectations. These expectations come from its exceptional fluid and rock properties – the total organic content (TOC) exceeds 2% throughout most of the formation, thickness ranges between 30–500 m, it is overpressured (providing energy for the production of hydrocarbons) and deep (2000–3500 m), ensuring the shallow (~400 m deep) aquifers will be safe during hydraulic stimulation. Moreover, the Vaca Muerta formation is located in an area that has historically produced oil and gas, making logistics easier (Askenazi et al 2013).

Estimating the potential size and production of an asset, along with its associated uncertainty, is crucial in decision-making. Underestimating forecasted production and reserves could lead to underinvesting in a good project and undervaluing the assets of the company. Overestimating forecasts and reserves can lead to problems with the Securities and Exchange Commission (SEC) and investors. This happened to Repsol YPF in 2006 when it announced it would reduce the reserves estimates published in 2005, having to pay a settlement of $8 million for a class action, which was reflected in a decrease in its stock price (Olsen, Lee, and Blasingame 2013). Over-forecasting can also hurt operators directly due to allocation of resources to underperforming projects. Probabilistic methods quantify uncertainty and can yield better decisions and results, as opposed to deterministic methods (Capen 2013). Reliable (unbiased) estimations of uncertainty can help optimize portfolios to obtain the most profitable outcomes (McVay and Dossary 2014).

The area overlying the Vaca Muerta formation has had oil and gas activity since 1918, with many well penetrations. Between 2006 and 2010, 302 study and exploratory vertical wells were drilled by various companies to characterize the reservoir and estimate its potential. When the development of the Vaca Muerta was launched in 2011, due to the thickness of the formation (up to 500 meters) and the lack of know-how to drill horizontal wells, first attempts at production were from vertical wells. After drilling 414 vertical wells between 2011 and 2015, their underperformance compared to the initial expectations, combined with the availability and lower costs of horizontal drilling technologies, plans to exploit the Vaca Muerta formation with vertical wells were abandoned. From 2015 onwards, only horizontal wells were drilled for development,

leaving new vertical wells for exploration and/or study purposes (obtaining core and/or fluid samples). In some cases, these wells were put into production through drilling of horizontal sidetracks, or hydraulic stimulation of the vertical section to recover some of the drilling costs.

Since 2011, 223 horizontal wells and 444 vertical wells have been drilled and completed targeting the Vaca Muerta formation, with varying results (Ministerio de Energia y Mineria de la Republica Argentina 2017). As more wells were drilled, some experienced spacing problems, which ended in fracture interference and burst pipes. While the spacing issues are still under study, and drilling and fracture designs keep changing (longer lateral lengths, introduction of geosteering and high-density completions, and changes in proppants for local alternatives), future reservoir performance is still uncertain.

1.2. Status of the question

Although there are frequent announcements in the newspapers with the latest updates of Vaca Muerta development and statements of potential reserves based on the first publication of the Energy Information Administration (EIA, 2011), as of March 2017, there have been few publications of studies estimating the technically-recoverable resources and/or reserves of the Vaca Muerta formation. While most of the studies are deterministic, there are some probabilistic assessments (**Table 1**).

Table 1—Summary of the published estimates of oil and gas reserves and resources in the Vaca Muerta shale

Author(s)	Type of classification	Oil, Bbbl				Gas, TSCF				Method
		Mean	P10	P50	P90	Mean	P10	P50	P90	
EIA (2011)	Technically recoverable resources	-	-	-	-	240	-	-	-	Analogs and volumetric method
YPF (2011)	Technically recoverable resources	-	40	-	-	-	117	-	-	Not specified
	Original oil in place (OOIP) and original gas in place (OGIP)	661	-	-	-	1181	-	-	-	
Gutierrez Schmidt et al. (2014)	Prospective resources	36.7	55.4	39.5	27.4	-	-	-	-	Probabilistic volumetric method
Stinco & Barredo (2014)	Technically recoverable resources	-	-	-	-	220	-	-	-	Volumetric method
EIA (2015)	Technically recoverable resources	16.2	-	-	-	307.7	-	-	-	Analogs and volumetric method

From the results in **Table 1**, it may seem that oil estimates steadily decreased over the years. This is more likely related to the type of classification investigated by the studies, rather than an overestimation in the earlier studies.

Here, technically recoverable resources (TRR) refers to "those quantities of petroleum producible using industry practices, regardless of commercial or accessibility considerations" (PRMS 2018). Prospective resources are those quantities of petroleum estimated, as of a given date, to be potentially recoverable from undiscovered accumulations by application of future development projects. Contingent resources are those quantities of petroleum estimated, as of a given date, to be potentially recoverable from known accumulations, but the applied project(s) are not yet considered mature enough for commercial development due to one or more contingencies (PRMS 2011). The sum of reserves, and prospective and contingent resources make up the TRR estimates.

In the estimates by the EIA (2011, 2015), Gutierrez Schmidt et al. (2014), and Barredo and Stinco (2014), the methodologies involved subjective recovery and risk factors that were applied to in-place estimates. Furthermore, Gutierrez Schmidt et al. (2014) recognized that the technically recoverable volumes estimated have significant uncertainty, which was not quantified. As for YPF's 2011 estimate, the methods used to calculate the estimates are not even described. The wide ranges of results indicate considerable uncertainty, and the significantly higher YPF OOIP and OGIP estimate could be due to a possible optimism bias. The other problems with all these studies are that they are outdated and were done early in the lives of the few existing horizontal wells. It has been four years when the latest study was done by the EIA in 2015. Back then, the

average life of the 77 existing horizontal wells was less than 12 months, and since then, the drilling and completion design has changed multiple times, thus changing well performance. Using short production histories from wells that have an outdated design leads to high uncertainty and wrong estimates. To my knowledge there is no publicly-available, play-wide assessment of oil and gas reserves and resources after 2015. The large and not-properly-assessed uncertainty and the possibility of bias in the available estimates, combined with the mentioned changes in drilling and completion methods, calls for a new probabilistic assessment of the reserves and resources.

As described by Morales Velasco (2013), there are different methodologies available to forecast production and estimate reserves and/or resources: material balance, analogy, volumetric analysis, reservoir simulation, and decline-curve analysis. The most appropriate methodology would depend on the information available and the nature of the reservoir. However, some of these methodologies have clear disadvantages and limitations when applied to the Vaca Muerta shale:

- Analogy: directly compares a reservoir to a known, older one, of similar geological and petrophysical properties to estimate the OOIP and the OGIP by assuming wells will have a similar performance to the ones of in the known reservoir. The Vaca Muerta shale is the first unconventional reservoir to be produced in Argentina. Although the updated Petroleum Resources Management System (PRMS) guidelines from 2011 do not require the analog reservoir to be in the same geographic area or be of a similar geologic age (Sidle and Lee 2010), it would still not be advisable to use any of the shale plays in North America as an analog for the Vaca Muerta given the differences in the petrophysics and rock properties (Askenazi et al. 2013). The lack

of a close analog would likely result in a large uncertainty and erroneous estimation of the calculated oil and gas TRR volumes. While this method is useful early in the life of a play, now that more historic production data are available, other methods will be able to provide better results.

- Volumetric Methods: require recovery factors and drainage areas, obtained from previous experience, to estimate reserves. Since there are no horizontal wells that have been fully produced to obtain real recovery factors, this method has a large associated uncertainty.
- Material Balance: needs accurate average reservoir pressure data, which is not available in the public dataset, making it unviable for this thesis.
- Reservoir Simulation: uses material balance and fluid flow equations. As mentioned previously, the available dataset does not provide all the necessary information to use material balance, and thus reservoir simulation.
- Decline-Curve Analysis (DCA): uses historic production data to forecast production and estimate reserves. There are various DCA methods available to account for the specific types of declines and flow regimes (Arps 1945, Valko and Lee 2010, Ilk et al. 2008, Duong 2013). Probabilistic methods can be used with these DCA methods to provide distributions of the forecasted oil or gas production, quantifying uncertainty (Gong et al. 2014).

In summary, excluding internal assessments from the companies operating in Vaca Muerta, which are not publicly available, it has been three years since the last published study. Moreover, this last study was conducted with little production data, resulting in

large uncertainties associated with the estimates. New production data and more geologic certainty from new wells drilled since 2015 should enable better estimations of reserves and resources.

1.3. Objectives

The objective of this research is to assess the reserves, and the contingent and prospective resources, of oil and gas in the Vaca Muerta formation, and to quantify the uncertainty in these assessments.

1.4. General approach

The reserves and resources in this study will be classified and categorized using the SPE PRMS guidelines (2011). Throughout the study, the term "area" refers to the gross area of interest that the Vaca Muerta formation covers, and the term "sub-area," refers to a smaller area defined within that gross area. This study had two major workflows given the available information and the considerations required for each of them.

The first workflow focused on sub-dividing the area overlaying the Vaca Muerta formation into sub-areas based on fluid type, and identifying the most appropriate DCA model for each of these sub-areas. To do so, a hindcast study was done using a selection of 58 horizontal and 85 vertical representative wells. These wells were considered representative because they use current well designs and did not experience any of the issues that have already been solved, like burst pipes due to fracture interference, or fracture damage due to poor proppant selection (crushing). To be selected, wells also needed to have at least 12 months of production history to allow for a better study of the most appropriate decline-curve model.

The second workflow estimated the reserves, and prospective and contingent resources for each of the sub-areas. Using the most suitable decline-curve model for each sub-area, an individual probabilistic-decline-curve analysis was conducted on each of the 177 (horizontal and vertical) wells targeting the Vaca Muerta formation which were still producing on January 1st, 2018, to estimate reserves. Gas production in the BO, VO, and WG sub-areas was calculated using a gas-oil-ratio (GOR) model in which gas increases slightly over time, developed in this thesis. To estimate prospective and contingent resources, probabilistic-type-decline curves and EUR distributions were created for each of the sub-areas following the recommendations from Freeborn and Russell (2016). In order to calculate the number of wells that would fit in each of the sub-areas, first, a map with all the existing wells (producing and abandoned) was created. Due to the lack of a published plan to drill them within the next 5 years, the production from offset wells that would fit within one section (640 acres) of existing wells was classified as contingent resources. The production from the wells that would fit in the remaining drillable area, outside the one-section surface, was classified as prospective resources. An economic analysis was done deterministically considering two scenarios: with and without the gas subsidies. The economic analysis would give more purpose to this study, if wells prove to be economic as it will increase the chances of new wells of being drilled. Uncertainty in well spacing and well length were modeled to account for the likelihood these variables change, as wells' horizontal lengths increase, and spacing changes as operators learn and optimize development practices. A more-detailed explanation of these variables and their distributions will be provided later in this paper.

2. GEOLOGY AND RESERVOIR CHARACTERIZATION

2.1. Regional geology

The Vaca Muerta formation extends throughout the center west part of Argentina, predominantly in the province of Neuquén, but also extending to the provinces of Río Negro, La Pampa, and Mendoza. The formation extends over 25,000 km^2 (6.18 million acres) of the Neuquén Basin.

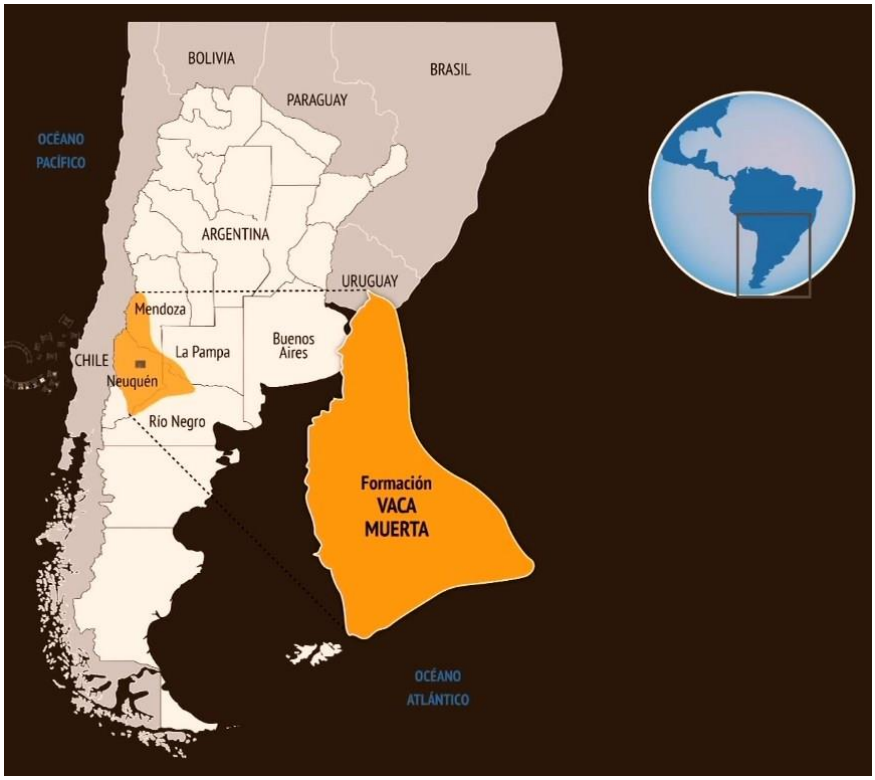

Fig. 1—Location of the Vaca Muerta formation (Reprinted from Vaca Muerta Info 2017)

The region has been exploited since 1918, when the first conventional oil and gas resources started being produced. The Vaca Muerta formation has been penetrated by thousands of wells, partially or totally, as part of the development of conventional reservoirs in the Neuquén basin. This development has enabled geologic characterization and has indicated the presence of hydrocarbons in the Vaca Muerta formation, although they were not commercial for production until the recent developments in horizontal wells and hydraulic fracturing.

2.1.1. Tectonic setting

The Neuquén basin has its origins at the western margin of Gondwana, and has been active since the Proterozoic (Ramos 1988). The basin was conditioned by flexural subsidence in most of its regions.

By the Permian-Triassic, the Neuquén basin had evolved to an extensional regime with the development of back-arc basins, creating engulfments. These deformations were favored by the geothermal gradient; due to the magnetism of the arcs and the relatively dense cortex, the resistance of the plate decreased (Lambias, Laenza, and Carbone 2007). The lower resistance allowed the development of a wide rift with deep faults, without becoming a basin or range (Buck 1991, Uliana, Biddle, and Cerdan 1989).

During the Pre-Cuyan phase, Neuquén basin was filled with continental clastic and pyroclastic deposits that filled it with asymmetric depocenters separated by transfer zones. The extension prolonged until the Jurassic, and it was reactivated during the Upper Triassic-Lower Jurassic (Barredo et al. 2008, Fernandez Seveso and Tankard 1995). The filling with marine and continental facies controlled by eustatic and tectonic variations of this stage corresponds to the Cuyo Group (Legarreta and Gulisano 1989). During this

time, the basin was subject to subsidence due to a second rift stage, which slowed down as it started cooling.

During the High Upper Triassic-Lower Jurassic, the zones close to the Huincul Dorsal suffered compression with inversion of old extensive structures (Barredo et al. 2008). As a result, the Oriental part of the basin stayed as a higher region, limiting marine inflows of the Molles Formation. This was followed by a general tendency of an increase in sedimentation compared to the creation of space, suggesting the basin was expanding due to thermal cooling (Cruz et al. 1999, Fernandez Seveso and Tankard 1995, Gulisano and Gutierrez Pleimling 1994).

Several episodes of inversion affected the submersion of the sag, which encouraged the development of continental and marine environments until the Paleocene. At this time, the Andean orogeny compressional regime started to control the subsidence through lithospheric flexion. The sedimentary environments in this stage were controlled by the mechanic characteristics of the flexed slab. Its elastic response to the tectonic pulses allowed the development of an extensive basin, with periods of low base levels and developments of prograding sequences. In the phase of tectonic stillness, the slab released the stresses as a viscoelastic medium, submerging the basin more. This was accompanied by a retrograding of the sequences during the marine transgressions of the Eustatic level rise, or from the development of fluvial lacustrine systems.

2.1.2. Structural setting

Identification of the fault system is crucial for avoiding problems while drilling (deviated wells) and fracturing (poor fracture propagation). Faults can also channelize fracture fluid during the hydraulic stimulation, which can cause the interference or *hit* of wells further

away than the usual fracture length, if they are bisected by the same fault as the stimulated well. Understanding the fault system helps plan for well shut-ins to prevent damage of wells during fracture hits, since by closing the offset wells, pressure builds up in them, helping ward off the hydraulic fracture.

There are two main structural regions that can be differentiated: the low deformed eastern zone, and the more complex western area (Sagasti et al. 2014). The eastern zone is characterized by a north-northwest (NNW) normal fault system. This fault system is the result of a low-angle convergence between the northwest stress regime and the west-northwest basement lineaments in the Early Jurassic (Sagasti et al. 2014). The maximum vertical displacement of these faults is about 295ft (90m) with a maximum throw of 197ft (60m). The western region develops within a transfer zone where the NNW normal fault converges with a north-northeast (NNE) reverse fault system (Sagasti et al. 2014). This NNE fault system is related to the local compressive stress at the tip of basement faults. The maximum displacement of these faults is under 50ft (15m). Last, there is an east-northeast (ENE) major lineament that extends several kilometers southwest from the transfer zone (Sagasti et al. 2014). This lineament is identified as a depression with changes in slope in seismic reflections. The ENE lineament, which was active until the end of the Early Cretaceous, affects the whole Quintuco-Vaca Muerta sequence, and is related to the uplift of the Huincul High.

2.1.3. Regional stratigraphy and depositional environments

The geological and petrophysical variations in the Vaca Muerta formation are linked to its geodynamic history. It has dark grey organic-rich shales, deposited in a deep-water environment in the western middle sections of the basin. These shales change laterally

and to the east to calcareous sandstones and limestones of a well-developed shelf. Towards the external ramp, the stratigraphy is characterized by a stacked rhythmic alteration of marls, black shales, and limestones that show the restricted depositional conditions (Barredo and Stinco 2014).

2.2. Resource occurrence

As presented by Gutierrez Schmidt et al (2014) in a study for the province of Neuquén, samples and analyses of a set of 129 wells and 9 outcrops in the area enabled the characterization of the resource occurrence in the Vaca Muerta formation, by providing data on the TOC and thermal maturity. These wells penetrated the Vaca Muerta shale targeting deeper formations.

2.2.1. Organic richness

The TOC in the Vaca Muerta formation ranges mostly from 3 to 8%. The highest values are found in the engulfment of the basin, decreasing towards the other parts of the basin. The Nor-Oriental Platform shows TOC ranges between 2–5% with some few exceptional areas showing 5–10% values (Stinco and Mosquera 2003). These organic-rich facies developed during the back-arc marine embayment, under anoxic conditions, in tune with the Jurassic-Cretaceous ups and downs of eustasy (Legarreta and Villar 2011). The center of the basin shows TOC ranges between 0.8 and 4%. Last, the Huincul Dorsal (south), shows TOC values that range between 3 and 4.5%. The contour map in **Fig. 2** shows the location of the previously mentioned areas and the TOC (%) throughout the Neuquén Basin. Vertically, TOC values range between 0.5–5% in the top half of the formation, called Superior Vaca Muerta, which has an average thickness of 200 m, and from 8–10% in the bottom part of the formation, called the kitchen, and which has between 30–35 m of thickness.

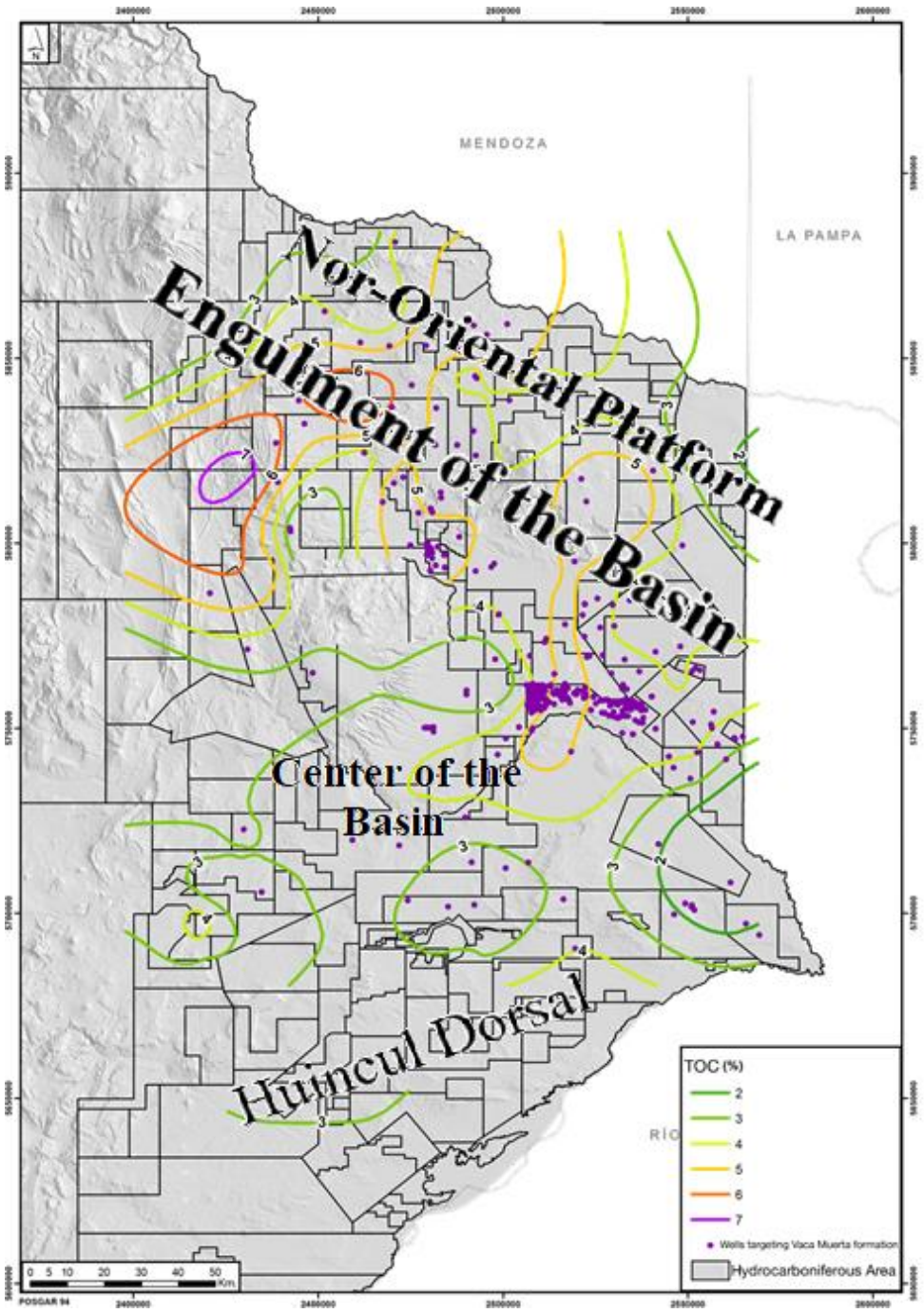

Fig. 2—TOC contour map (after Gas y Petroleo del Neuquén 2018)

2.2.2. Thermal maturity and kerogen types

The maturity of the source rock was obtained through pyrolysis analysis. The kerogen identified in the Nor-Oriental region of the source rock is a mix of Type I and II linked to the algal contribution with little to no terrestrial contribution. This kerogen composition indicates high potential for liquid hydrocarbons. This region was considered marginally to prematurely thermally mature, entering the generation zone towards the deepest parts of the formation (Stinco and Mosquera 2003). In the center of the basin, kerogen Type II and Type III were found, with the thermal maturity in the main window for oil and gas. Towards the Huincul Dorsal, Type I and Type II kerogen were found, with some Type II-S facies towards the marginal regions, showing a high capacity for generating liquid hydrocarbons. In this region the kerogen was found to be thermally immature (Legarreta et al. 2005). The contour map in **Fig. 3** shows the average vitrinite reflectance (Ro, %) as a proxy for thermal maturity in the areas mentioned above.

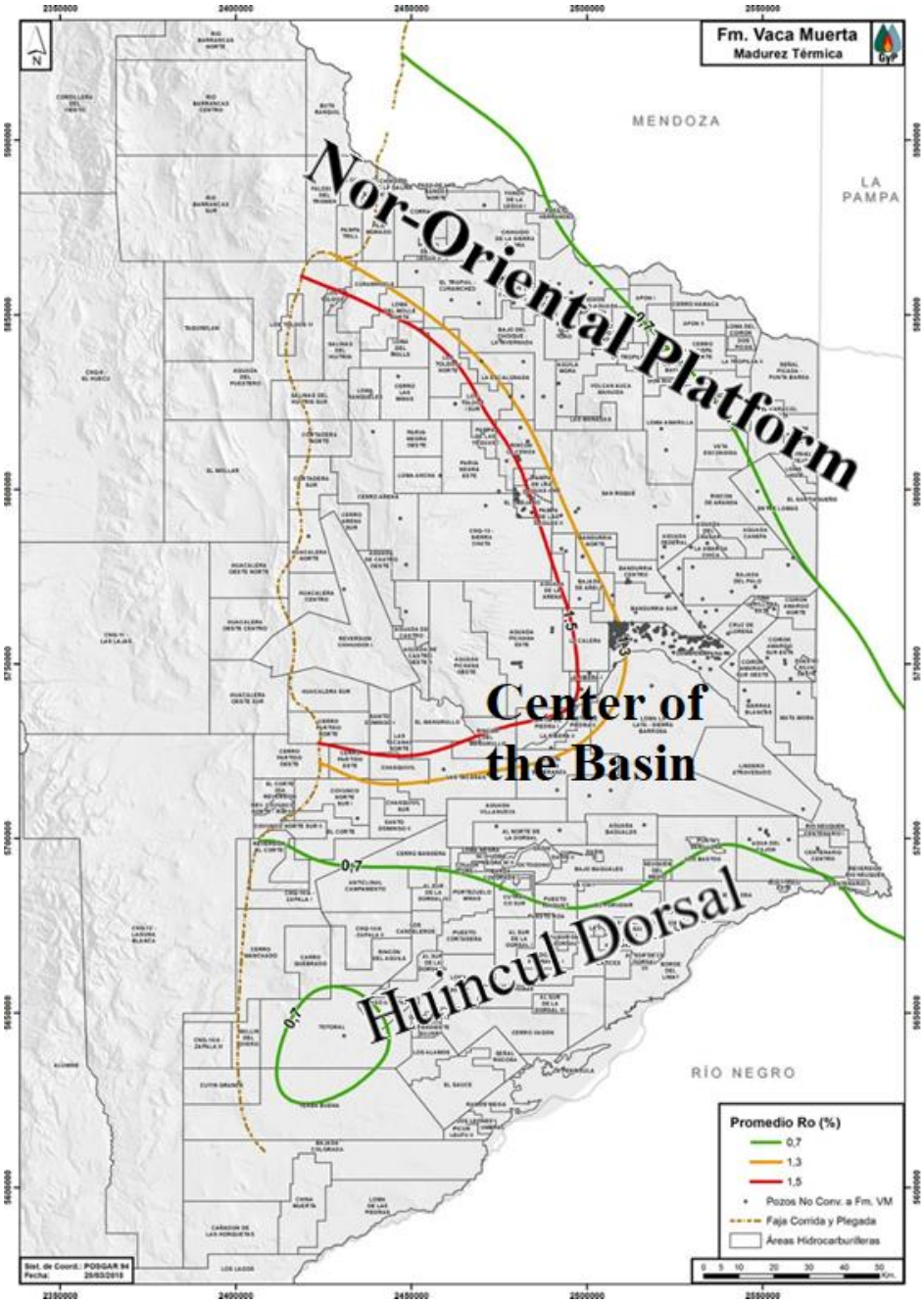

Fig. 3—Thermal maturity contour map, average vitrinite reflectance (Ro, %) (after Gas y Petroleo del Neuquén 2018)

2.3. Area prioritization and subdivision

The area overlaying the Vaca Muerta formation was analyzed and divided, based on reservoir fluid type: black-oil, volatile oil, retrograde condensate, wet gas, and dry gas (**Fig. 4**).

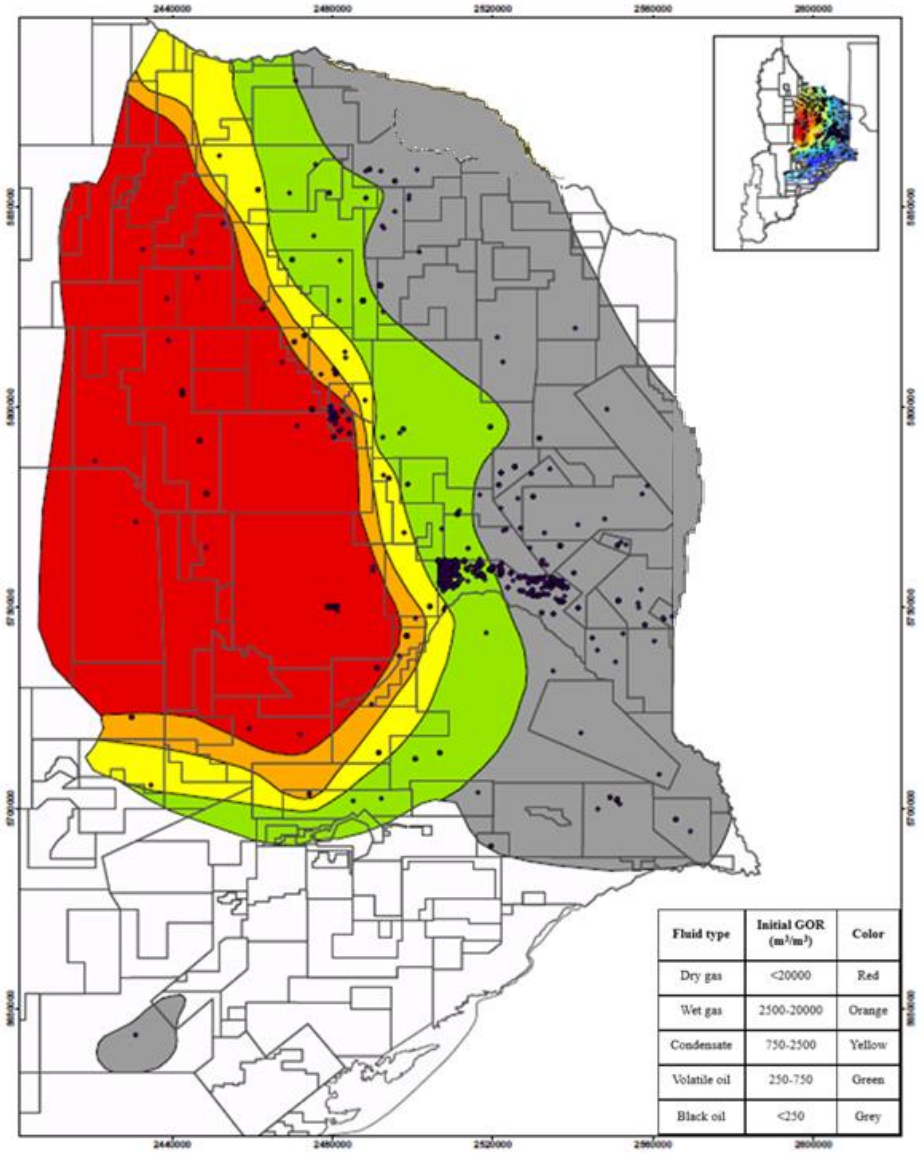

Fig. 4—Expected fluid type based on initial GOR (after Subsecretaria de Energia Mineria e hidrocarburos 2017)

Minimum cutoff values were established for TOC, formation thickness, and maturity level (**Table 3**) based on the performance of the exploratory wells. These cutoffs eliminate the regions with the least chances of being successful (Askenazi et al 2013). Depth is usually another variable taken into consideration to guarantee a safe distance from the aquifers (located ~400 m deep in the Neuquén basin). In this thesis, depth was not considered as one of the cutoff variables since the Vaca Muerta is deep enough throughout its whole area to keep aquifers safe. Using the contour maps in **Figs. 2, 3, 4** and **5** of TOC, thermal maturity, expected fluid types and thickness of the Vaca Muerta formation, respectively, combined with the cutoff values in **Table 2**, **Fig. 6** was obtained. **Fig. 6** shows the location and extension of the defined prospective areas, divided by PVT properties. The wet gas and retrograde condensate sub-areas were combined because they are similar in their geologic properties and there are not enough wells in each of them to create representative type-decline curves. A description of each of these areas is shown in **Table 3.**

Table 2—Minimum cut-off values

Variable	Cut-off value
TOC	2%
Formation thickness	164 ft (50 m)
Maturity	Mature

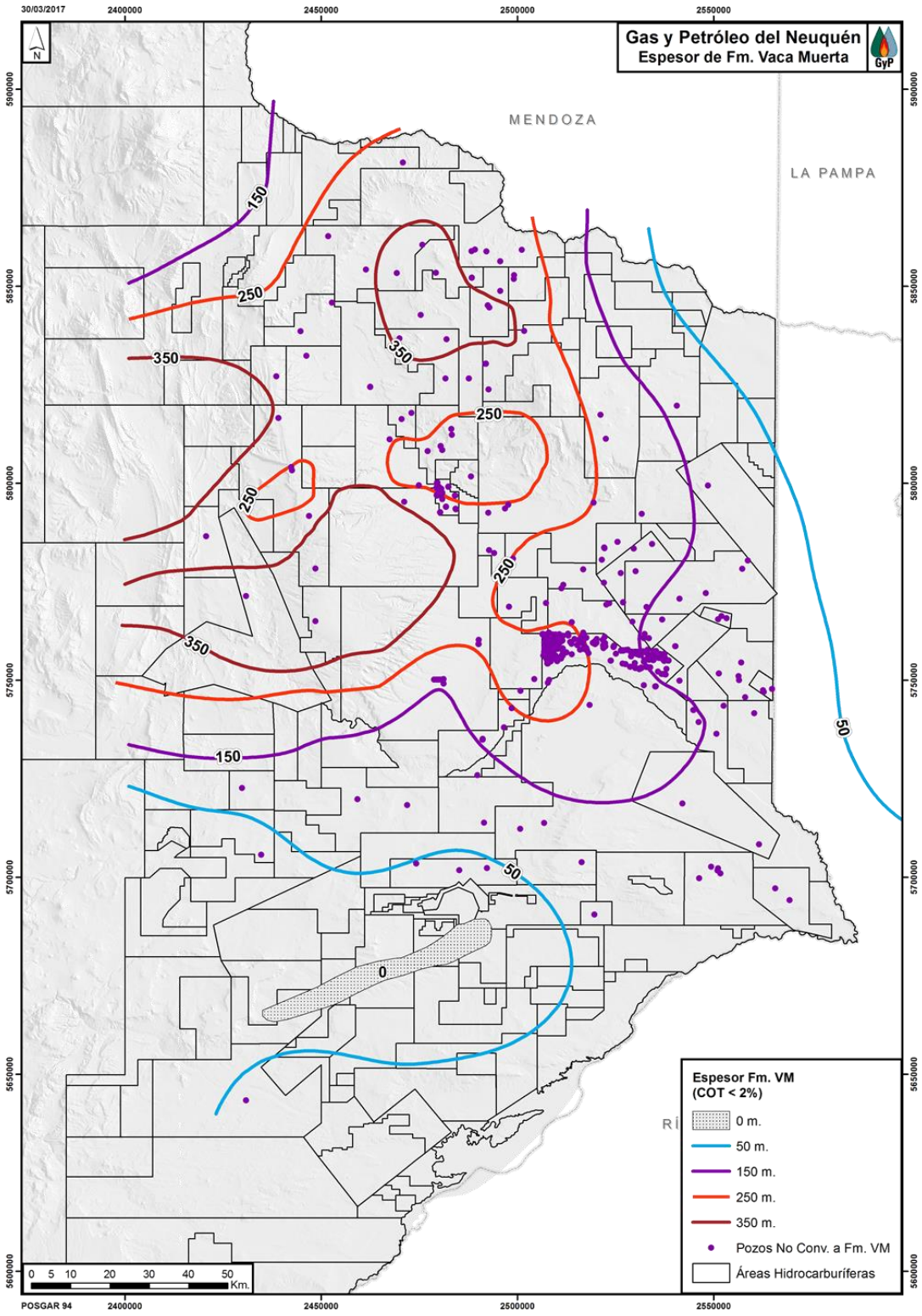

Fig. 5—Vaca Muerta formation thickness (in meters) (Reprinted from Gas y Petróleo del Neuquén S.A. 2018)

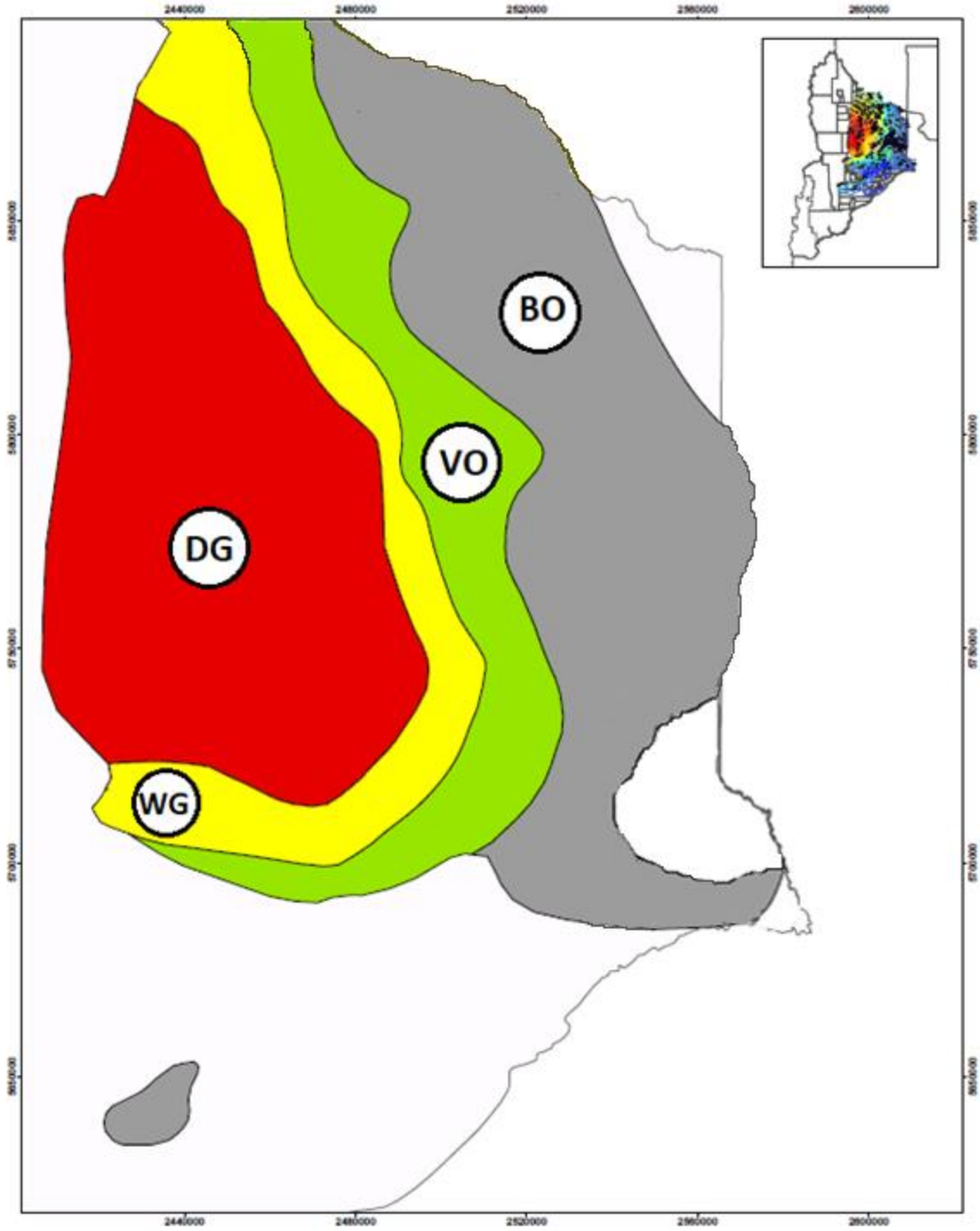

Fig. 6—Final prospect sub-areas

Table 3—Characteristics of the defined sub-areas in Vaca Muerta

	Defined sub-areas			
Variable	**BO**	**VO**	**WG**	**DG**
Location	Eastern part of the basin, surrounding sub-area VO	Center part of the basin, surrounding sub-area WG	Center-west part of the basin, surrounding sub-area DG	Northwestern part of the basin
Area	2.9 MM acres (11,860 km^2)	916 M acres (3,705 km^2)	593 M acres (2,400 km^2)	2.2 MM acres (8,900 km^2)
Average TOC	2.8%	3.4%	3.5%	3%
Maturity in terms of vitrinite reflectance (Ro%)	Mature. 0.6 – 1.1%	Mature. 1.1 – 1.3%	Mature. 1.2 – 1.5%	Mature. <1.5%
Thickness	509 ft (155 m)	1,086 ft (331 m)	1,296 ft (395 m)	1,804 ft (550 m)
Depth	7,874 ft (2,400 m)	9,186 ft (2,800 m)	9,514 ft (2,900 m)	10,499 ft (3,200 m)
Fluid type	Black oil	Volatile oil	Wet gas and condensate	Dry gas

3. PROBABILISTIC DECLINE-CURVE ANALYSIS REVIEW

Probabilistic decline-curve analysis (PDCA) can be done using available production data to forecast oil and gas production, and quantify the uncertainty of these estimates, which is important in shale plays with their heterogeneities and their capital-intensive nature. Quantifying risk and uncertainty is particularly relevant for the Vaca Muerta formation, given the early stage of development and the high expectations put on it to end the energy crisis Argentina is going through (Caraballo, Sacchetta, and Acosta 2016). Furthermore, the lack of publicly available data necessary to perform a reservoir simulation study, and the higher uncertainties associated with material balance, volumetric, and analogy methods, made the PDCA method the best choice for this thesis.

3.1. Probabilistic-decline-curve-analysis models

3.1.1. Decline-curve models for shales

Production decline-curve analysis uses measured production to forecast future production. Until production of unconventional resources started, the equations presented in Arps (1945) were the undisputed standard decline model. Since the model assumes boundary-dominated flow (BDF), it cannot be used directly for shale wells. Since most shale wells tend to spend years in transient-flow before reaching BDF, using the traditional Arps model would overestimate production and reserves.

Several models have been published since the increase in popularity of unconventional plays: Duong (2013), stretched-exponential (Valko and Lee 2010), and power-law (Ilk et al. 2008). Due to the short production history of most unconventional plays, and the large heterogeneities between the different plays and within the same plays, none of these models has become the standard. Despite multiple studies carried out to determine which

model is the most accurate for shale oil and gas production forecasting (Ali and Sheng 2015, Boulis et al. 2013, Gonzalez 2012, Joshi 2012, Kanfar and Wattenbarger 2012), there is still no consensus on which model will consistently yield the most accurate forecasts.

3.1.2. Probabilistic methodology

The wide range of outcomes obtained in the exploitation of shale resources make these resources perfect candidates for using a probabilistic approach to estimate production of oil and gas. Due to the advantages of probabilistic methodologies for assessing uncertainty, there has been an increase in adoption of probabilistic methods over the past decades (Murtha 2006). This went in hand with the frequent ups and downs in the industry, which made companies look for safer investments.

Markov Chain Monte Carlo (MCMC) simulations, a Bayesian methodology introduced by Gong et al. (2011), can quantify reserves uncertainty "reliably, quickly and without modifying historical production data" (Gong et al. 2011). This methodology, parameters of the decline-curve models are assumed to be random variables. A Markov chain of the decline-curve parameters is constructed using MCMC with the Metropolis algorithm (random walk). This Bayesian methodology can be applied to decline-curve analysis to estimate the probability distributions of parameters with production history data since it "samples on time t based only on the sample drawn at time t-1 and not any sample drawn before that" (Morales Velasco 2013). According to a study done by Gong et al. (2014), this methodology successfully quantified uncertainty, providing narrow P90–P10 ranges when analyzing horizontal fractured wells from the Barnett shale, fast (taking, on average, 10 seconds to analyze one well). The performance of the MCMC simulations is

expected to be equally good when used in the Vaca Muerta formation, since the methodology is not linked to the geological properties of the formation.

MCMC was validated in Gonzalez's (2012) thesis, obtaining reliable results. More importantly, Gonzalez showed the MCMC methodology can be coupled with the decline-curve models proposed for the analysis of Vaca Muerta in this thesis.

3.2. Data acquisition

Monthly production data through January 2018 was gathered from the Ministry of Energy's exploration and production per year database (Ministerio de Energia y Mineria de la Republica Argentina 2018). In Argentina, production data is reported for each individual well. A total of 151 wells that satisfied the following criteria were selected to find the most appropriate decline-curve model for each sub-area in the following section:

- Initial production after 1/1/2011 to include only the wells from the development stage.
- Produced from the Vaca Muerta formation.
- Horizontal and vertical wells.
- Smooth production data.

Data in this dataset are always uploaded by the operators. Some companies publish the monthly production in m^3/day while others publish in m^3/month, so quality checks were made manually to ensure consistency in the units.

3.3. Finding the most appropriate decline-curve model

Since no study has been done to determine the most appropriate decline model for the Vaca Muerta formation, this thesis will first investigate the performance of the Arps (1945), Duong (2013), power-law (Ilk et al. 2008), and stretched-exponential (Valko and

Lee 2010) models. As described by Gong et al. (2014), the best way to determine which decline-curve model to use is through a hindcast. Wells with more than twelve months of production data were selected from the 4 sub-areas: BO, VO, WG, DG. **Table 4** and **Fig. 7** show the number of wells selected in each sub-area and the location of selected wells, respectively. The hindcast was done separately for vertical and horizontal wells. Finding the most appropriate decline-curve model for horizontal wells will be useful for almost all future wells. Finding the most appropriate model for vertical wells will ensure that the correct model is used to forecast reserves of the vertical wells that are still producing. For the BO, VO, and WG sub-areas, oil production was analyzed. For the DG sub-area, gas production was analyzed.

Table 4—Number of selected wells per sub-area

Sub-area	Vertical wells	Horizontal wells
BO	21	22
VO	29	25
WG	5	6
DG	15	28

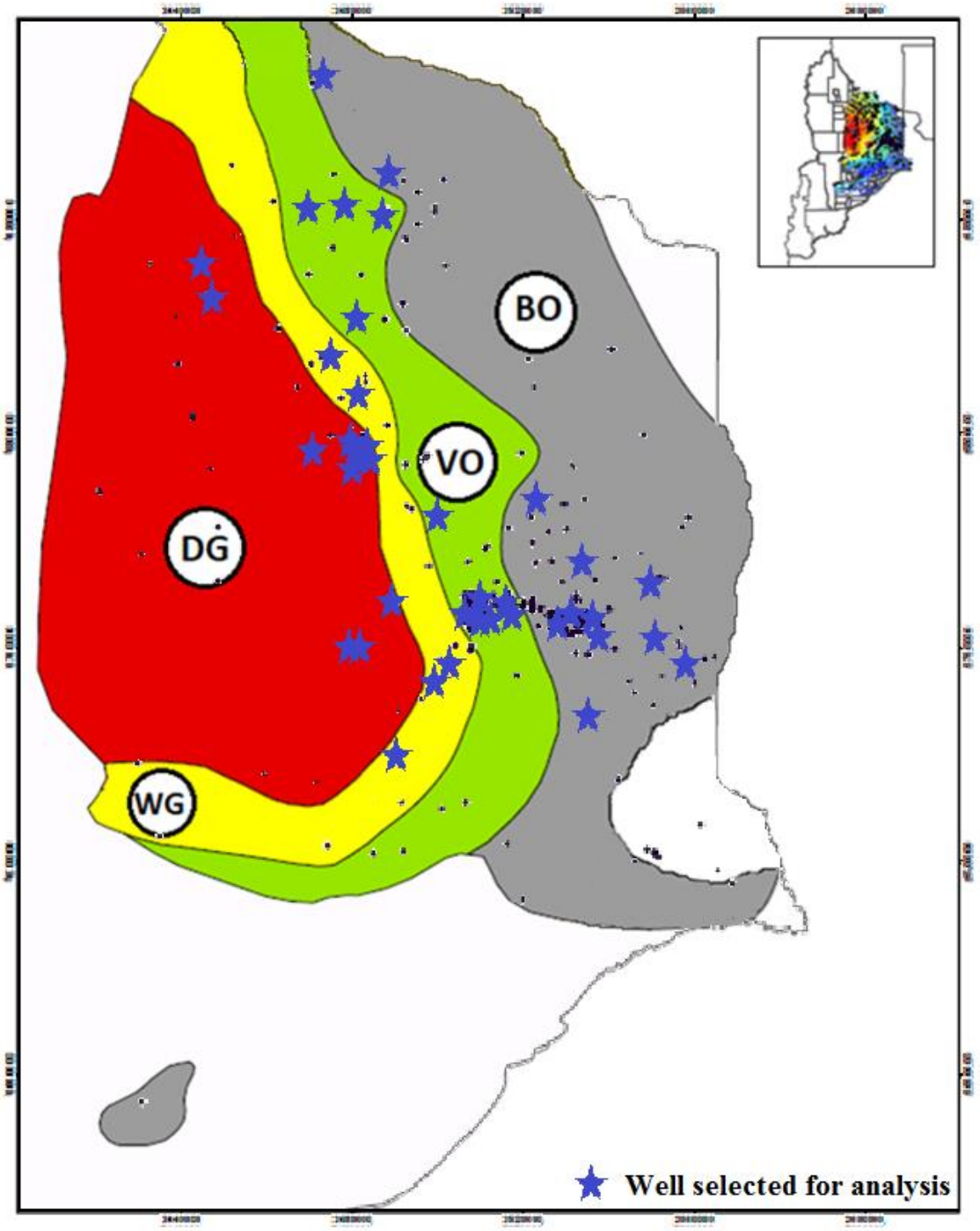

Fig. 7—Location of the wells selected for decline-curve study.

Following the methodology presented by Gong et al (2013), in the hindcast, the first 6

months of production were assumed known and the production during the second period (PDTSP) was compared with the hindcasted PDTSP using different decline-curve models combined with MCMC. Although long-term forecasting of a well´s production is not recommended with only 6 months of data, it is the maximum time that could be used for the selected methodology given the short production time of the majority of the horizontal wells. While this might lead to identifying the wrong model as the most appropriate for the long-term forecasting, it is the best that can be done with the available data, given that 79% of the 696 existing wells had fewer than twelve months of production available.

To assess the prediction accuracy for the set of wells in each sub-area, the calibration score was used, by calculating how closely the magnitudes of the assigned probabilities (P10, P50, and P90) track the relative frequency of the observed outcomes of the simulation. The results of the hindcasts were plotted as proportion correct versus the probability assigned, where the desired result is that the proportion correct equals probability assigned for the entire distribution. The proportion correct of the P10, P50, and P90 estimates were calculated as the fraction of wells out of the total used in each hindcast for which the actual PDTSP was larger than the P10, P50, and P90 PDTSP estimate respectively. The calibration score was calculated as the average distance of the proportion correct curve to the probability assigned curve. The average coverage rate was also calculated as a secondary point of comparison. This average coverage rate was calculated as the fraction of wells of the total evaluated for which the actual PDTSP falls within the P90–P10 range predicted by the model. The model with the lowest calibration score and the highest coverage rate was selected for the DCA to estimate reserves and type-decline curve creation.

The first model tested was the Arps (1945) model. This empirical model is more reliable when used at high drawdown, during the BDF period. To analyze the different flow regimes throughout the life of the well, this model can be used in segments.

The flowrate equation of this model under exponential decline *(b*=0) is:

$$q = q_i e^{-dt}$$

The flowrate equation of this model under hyperbolic decline (0<*b*<1) is:

$$q = \frac{q_i}{(1 + bd_i t)^{1/b}}$$

The flowrate equation of this model under harmonic decline (*b*=1) is:

$$q = \frac{q_i}{(1 + d_i t)}$$

The parameters of this model are:

- q_i: the initial production rate, in m^3/month [vol/time].
- d_i: the initial nominal decline rate, in 1/month [1/time].
- *t*: cumulative time since start of production, in months [time].
- *b*: the hyperbolic decline constant.

The second model tested was the Duong (2013) model. This model assumes long-term linear flow and no boundary effects during the entire well life. This assumption would imply overestimating production and reserves. To avoid this, a minimum-decline-rate was imposed by shifting to Arps exponential decline, as Morales Velasco (2013) did.

The flowrate equation of this model is:

$$q = q_1 t^{-m} e^{\frac{a}{1-m}(t^{1-m}-1)} + q_\infty$$

The parameters of this model are:

- q_1: flow rate at day 1, in m^3/month [vol/time].

- t: cumulative time since start of production, in months [time], instead of days in the original model (Duong, 2013) because of the monthly production data used for this study.
- -m: is the negative slope of the straight line of the log-log plot of q/G_p vs t for gas, or q/N_p vs t for oil.
- a: is the is the intercept of the straight line of the log-log plot of q/G_p vs t for gas, or q/N_p vs t for oil.
- q_∞: rate at infinite time, in m^3/month [vol/time].

The q_1 parameter is found by plotting q against $t^{-m}e^{\frac{a}{1-m}(t^{1-m}-1)}$. This plot should be a straight line going through the origin with a slope of q_1.

The third model tested was the power-law decline model introduced by Ilk et al. (2008). This model was created to forecast production of tight gas reservoirs. It can be used to model transient, transition, and BDF.

The flowrate equation of this model is:

$$q = \widehat{q_i}\exp\left[-D_\infty t - \widehat{D_i}t^n\right]$$

The D-parameter equation is:

$$D = D_\infty + D_1 t^{-(1-n)}$$

The parameters of this model are:

- $\widehat{q_i}$*:* rate intercept defined by the flowrate equation, *q(t=0),* in m^3/month [vol/time]
- D_1: decline constant intercept at 1 month, *D(t=1 month).*
- D_∞: decline constant at "infinite time", *D(t=∞).*
- *t*: cumulative time since start of production, in months [time].

- $\widehat{D}_i$: decline constant defined by the D-parameter equation, $\widehat{D}_i = D_1/n$.
- n: time exponent, defined by the D-parameter equation.

The last model evaluated was the stretched-exponential decline (SEPD) model presented by Valko and Lee (2010). This model is intended for transient data of low permeability oil and gas reservoirs and will provide a conservative estimate of oil and gas production when in BDF.

The equation for flowrate of this model is:

$$q = q_i \exp\left[-\left(\frac{t}{\tau}\right)^n\right]$$

The parameters of this model are:

- q_i: the initial production rate at *t=0*, in m^3/month [vol/time].
- τ: characteristic time parameter for SEPD model, in months [time].
- *t*: cumulative time since start of production, in months [time].
- n: exponent parameter for SEPD model.

Fig. 8 and **Fig. 9** present the combined results of the hindcast studies for horizontal and vertical wells, respectively, of all models for each sub-area. **Tables 5** and **6** present a summary of the results shown in the plots for horizontal and vertical wells respectively.

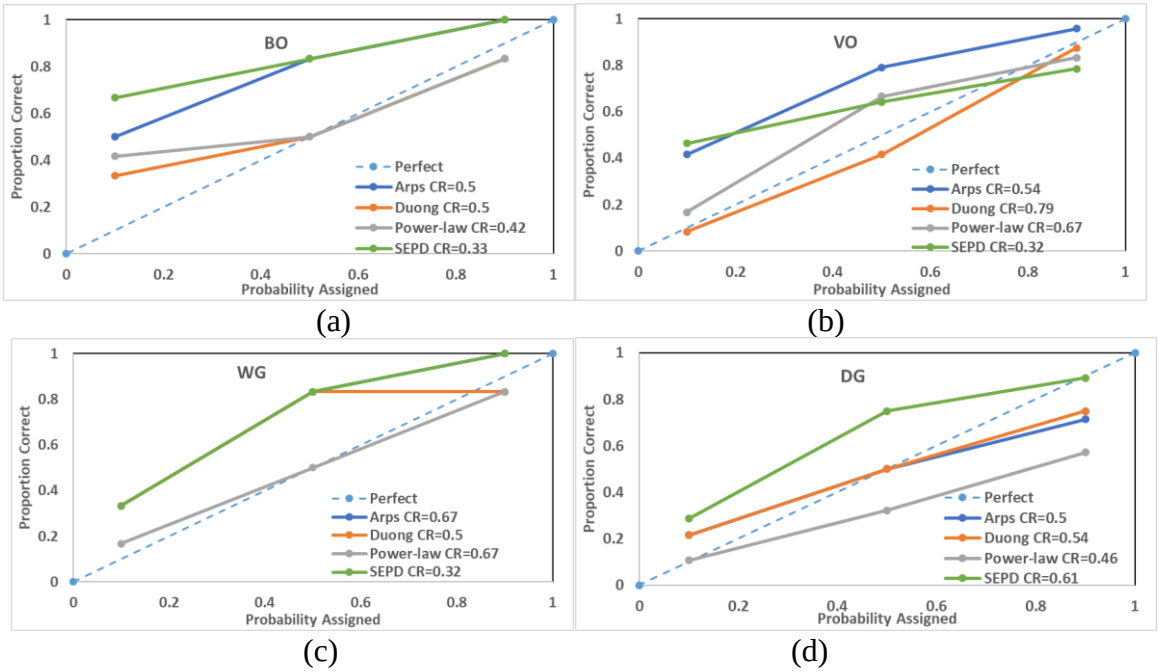

Fig. 8—Summary of the production hindcasts of black-oil sub-area BO (a), volatile-oil sub-area VO (b), wet gas and condensate sub-area WG (c), and gas production of dry-gas sub-area DG (d) for horizontal wells.

Table 5—Summary of results for all models, in all four sub-areas, for horizontal wells.

		Arps	Duong	Power-law	SEPD
BO	Calibration score	0.28	0.10	0.13	0.33
	Coverage rate	0.50	0.50	0.42	0.33
VO	Calibration score	0.22	0.04	0.10	0.21
	Coverage rate	0.54	0.79	0.67	0.32
WG	Calibration score	0.22	0.21	0.04	0.22
	Coverage rate	0.67	0.50	0.67	0.32
DG	Calibration score	0.10	0.09	0.17	0.15
	Coverage rate	0.50	0.54	0.46	0.61

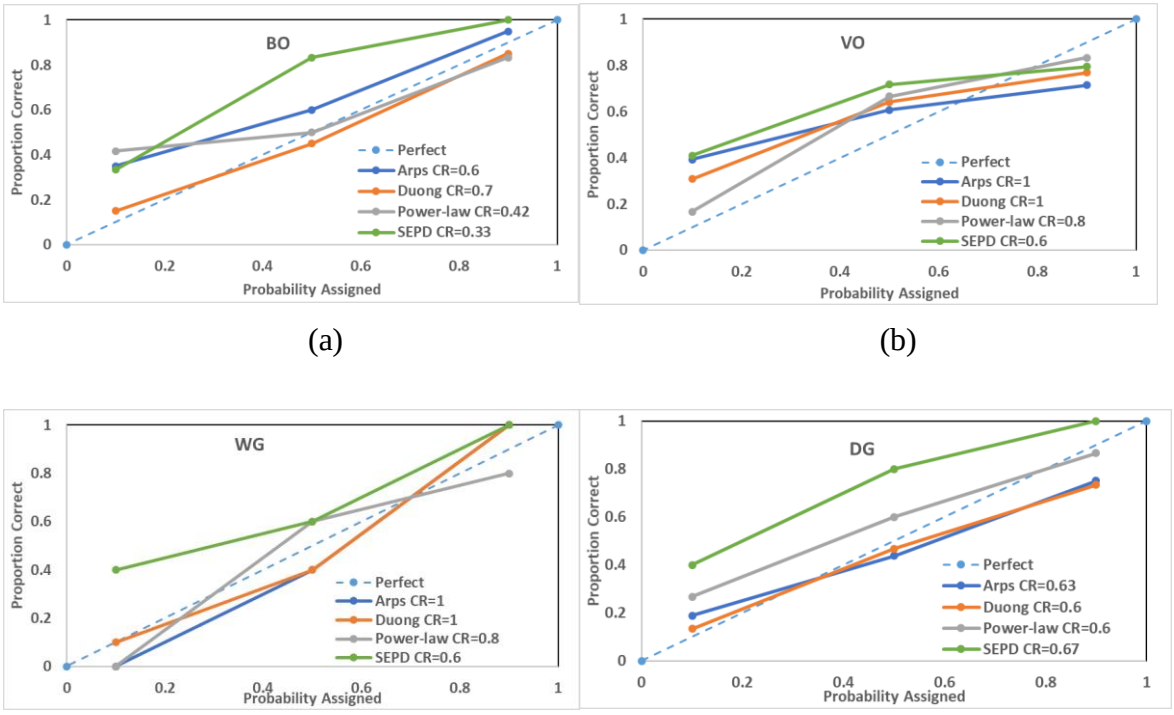

Fig. 9—Summary of the production hindcasts of black-oil sub-area BO (a), volatile-oil sub-area VO (b), wet gas and condensate sub-area WG (c), and gas production of dry-gas sub-area DG (d) for vertical wells.

Table 6—Summary of results for all models, in all four sub-areas, for vertical wells.

		Arps	Duong	Power-law	SEPD
BO	Calibration score	0.13	0.05	0.13	0.22
	Coverage rate	0.60	0.70	0.42	0.33
VO	Calibration score	0.20	0.16	0.10	0.21
	Coverage rate	1.00	1.00	0.80	0.60
WG	Calibration score	0.10	0.07	0.10	0.17
	Coverage rate	1.00	1.00	0.80	0.60
DG	Calibration score	0.10	0.08	0.10	0.23
	Coverage rate	0.59	0.60	0.60	0.67

Based on the results shown in **Table 5**, it can be concluded that for performing a decline-curve analysis of the horizontal wells in the Vaca Muerta shale the Duong model is the most appropriate for BO, VO, and DG with coverage rates of 0.5, 0.79, and 0.54, respectively, and the power-law model is the most appropriate for WG, with a coverage rate of 0.74. Similarly, from **Table 6**, it can be concluded that for performing a decline-curve analysis of the vertical wells in the Vaca Muerta shale the Duong model is the most appropriate for BO, WG, and DG, with coverage rates of 0.7, 1, and 0.6, respectively, and the power-law model is the most appropriate for VO, with a coverage rate of 0.8. The decline models that predicted oil/gas production more accurately in each of the sub-areas and well types, will be used for the estimation of reserves and creation of type curves in Chapter 5.

4. RESERVES

4.1. Applicable wells

As of January 2018, 746 vertical wells and 223 horizontal wells have been drilled targeting the Vaca Muerta formation with various results. Of these wells, 150 horizontal and 27 vertical wells are still producing (**Table 7**). To estimate reserves probabilistically for these producing wells, MCMC simulations coupled with the decline-curve models established in the previous chapter were performed for each sub-area and well type (horizontal or vertical). A minimum decline was imposed using the criteria that will be explained in this chapter to account for BDF. Initial GOR values and their monthly increase were modeled using data from existing wells in the BO, VO, and WG sub-areas to estimate gas production in each of these sub-areas. Aggregation of the estimates for each well within the same sub-area was done assuming both correlation coefficients of 0 and 1 to model both scenarios of full independence and full dependence between wells. Aggregation of reserves estimates across sub-areas was done arithmetically, following PRMS Guidelines.

Table 7—Producing wells as of January 2017

Sub-area	Vertical wells	Horizontal wells
BO	6	21
VO	10	83
WG	3	2
DG	8	44

4.1.1. Minimum decline assumptions

When estimating reserves, most of the operators developing the Vaca Muerta shale use a deterministic approach to minimum decline, to model production during BDF. The standardized rule in these companies is to switch to exponential decline when wells reach a determined nominal decline rate, ranging between 9 and 30%, depending on the company, fluid type, and well design[1]. Since these companies do not want the exact values they use for minimum decline to be disclosed, and this thesis wants to provide probabilistic reserves estimates, a model for the minimum decline will be created in this section.

The switch between flow regimes does not happen in all wells at the same time and it depends on several variables like fluid properties, pressure, fracture length and width, and permeability. Because of this reason, the minimum decline rate at which the decline model should switch to Arps exponential decline, during BDF, will be modeled as a random variable. To model the minimum decline rate during BDF, Gong (2013) modeled the distribution of decline rates of existing wells that had entered BDF. There are two problems using this methodology in the Vaca Muerta formation: there are not many wells that have reached BDF given the short production history from the formation, and there have been changes in well design (e.g., from vertical to horizontal, increase in lateral length, fracture stages) over the past years, which would change the distribution of the minimum decline rate. Therefore, to model the minimum decline rate:

1. A PDCA of the wells selected for the hindcast study in the previous chapter was performed, with no minimum decline.

[1] Personal communication with YPF, Shell, Tecpetrol, and Vista staff 2018. Neuquén, Argentina.

2. A uniform distribution for the time to BDF between 1 and 4 years was assumed based on the different simulations of the companies producing from the Vaca Muerta shale[2].
3. A MC simulation was performed to pick the nominal decline rates of the well PDCA forecasts, at the different random times to BDF selected from the uniform distribution mentioned before.

The minimum decline rate distribution (**Fig. 10)** was found to be a lognormal distribution with mean and standard deviation of 0.33 and 0.18 for gas wells, and 0.32 and 0.16 for oil wells. The higher mean minimum decline rate, compared to the ones used by most companies producing from the Vaca Muerta shale, should result in a more conservative estimate. Until more production data becomes available over time, from more wells, this is the best estimate for the selected methodology.

[2] Personal communication with YPF, Shell, Tecpetrol, and Vista staff 2018. Neuquén, Argentina.

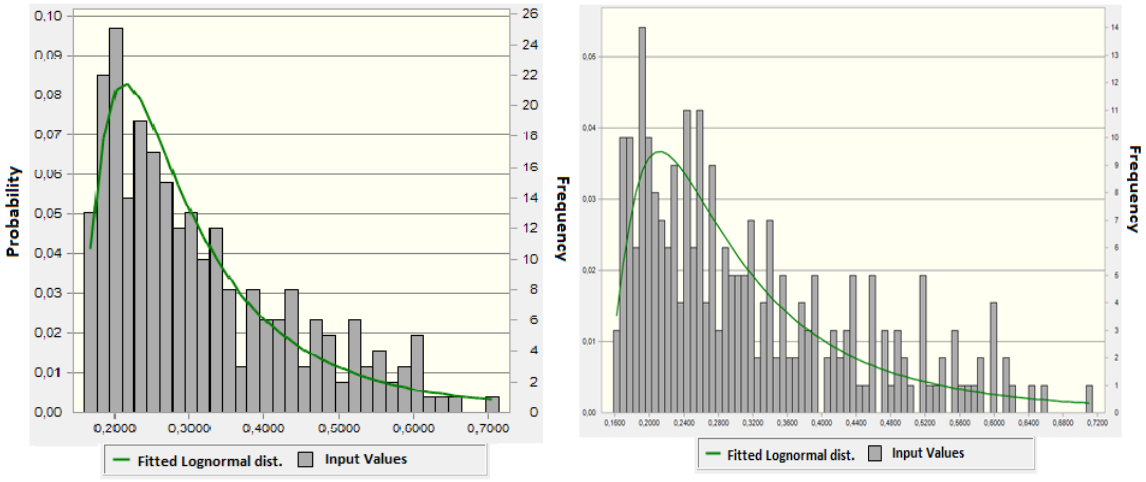

(a) (b)

Fig. 10—Probability distribution of the nominal decline rate for (a) oil wells and (b) gas wells when reaching BDF

4.1.2. Gas production forecasting

Generating a production forecast for horizontal, hydraulically fractured, wells with two-phase flow is complicated due to the changes in phases and relative permeability. Two-phase flow is observed in the Vaca Muerta formation in sub-areas BO, VO, and WG. As explained in the previous chapter, oil production was forecasted using PDCA. To estimate the associated gas production, a GOR model was used for each sub-area. To create the GOR models, first, oil and gas production profiles of all horizontal wells with drilling and completion designs similar to current designs were normalized to the same starting month. Then, gas production was divided by oil production for each month, to obtain the GOR. Last, the GOR of all wells in each sub-area was averaged for each month, and two straight lines to bracket the majority of the data were fit (**Fig. 11**). The last data points were ignored because the well count is significantly lower in the later months than

in the earlier months. GOR slope might change after the last available data points, but it is impossible to know at this time. The slopes of the two straight lines for each sub-area are summarized in **Table 8**. The GOR slope will later be sampled as a uniform distribution, ranging between the lower and the higher slopes.

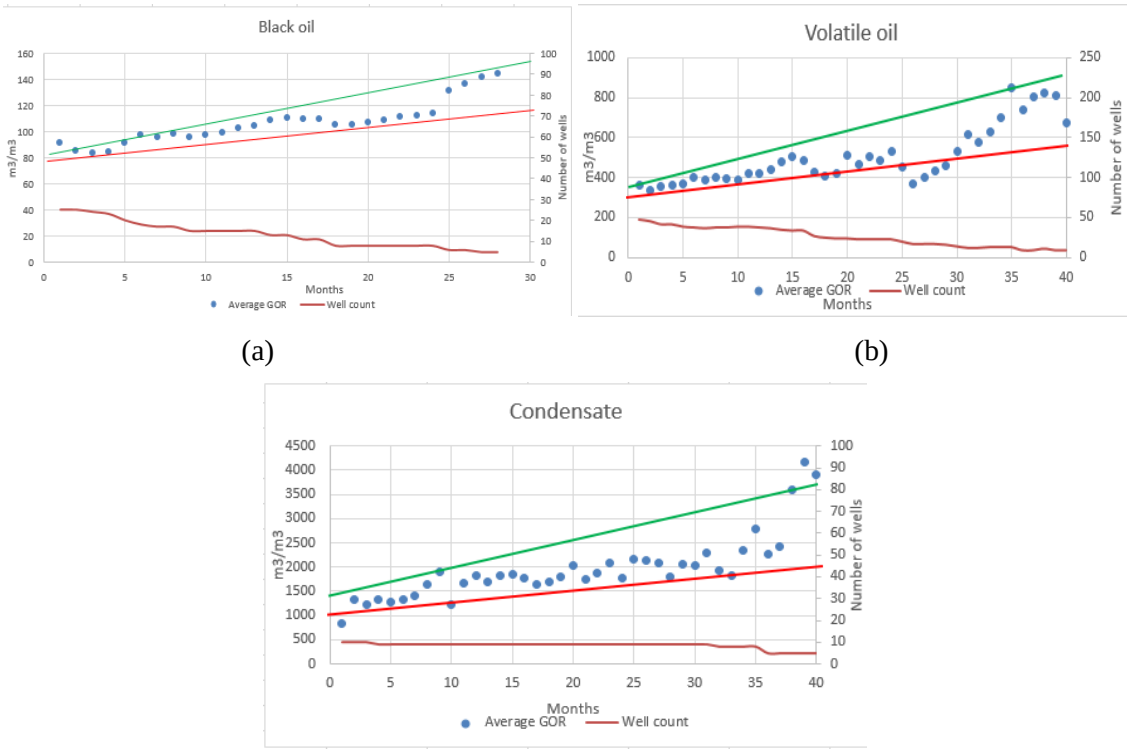

Fig. 11—Average GOR and the straight-line GOR models for (a) BO, (b) VO, and (c) WG

Table 8— GOR slopes for the three sub-areas BO, VO, and WG

Sub-area	Lower slope, m^3/m^3/month	Higher slope, m^3/m^3/month
BO	1.3	2.4
VO	5.7	13.3
WG	12.5	57.1

The initial GOR was also compiled for all wells in the BO, VO, and WG sub-regions. A lognormal distribution for the initial GOR in each sub-area was created (**Fig. 12**). The means and standard deviations of the distributions are shown in **Table 9**.

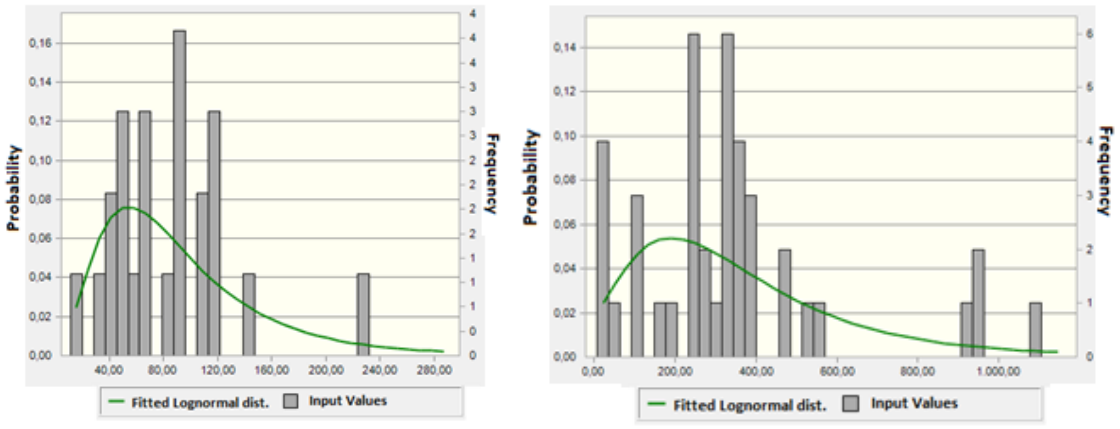

(a) (b)

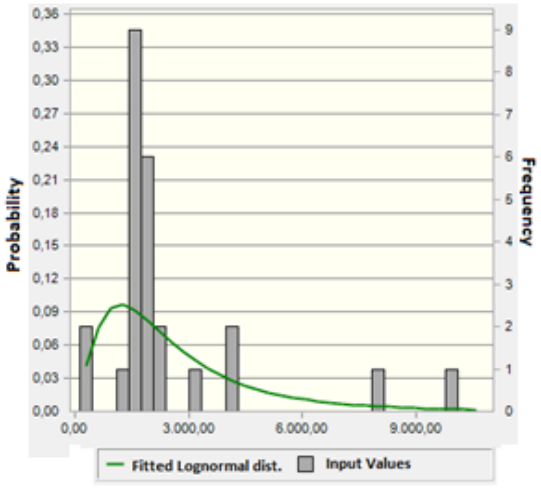

(c)

Fig. 12—Probability distribution of the initial GOR for (a) BO, (b) VO, and (c) WG

Table 9— Initial GOR distributions for the three sub-areas BO, VO, and WG

Sub-area	Mean, m^3/m^3	Standard deviation, m^3/m^3
BO	94.9	65.4
VO	363.3	9.0
WG	1,614.5	6,386.6

To forecast gas production and estimate gas reserves of oil wells in BO, VO, and WG:

1. After forecasting oil production, select a well from the existing producing wells.
2. Sample an initial GOR from the distribution in **Table 9** and a slope from the uniform distribution in **Table 8** to create a GOR model.
3. Multiply the GOR for the corresponding month by the forecasted monthly oil, to estimate gas production.
4. Repeat for all oil wells.

4.2. Aggregation methodology

For the aggregation of production between wells, the P10, P50, and P90 production can be summed arithmetically or probabilistically. While the first methodology assumes complete dependence between the production of wells in each sub-area, the latter assumes complete independence if the correlation coefficient is 0. As explained in Gong´s (2013) paper, the performance of wells in the same sub-area, sharing the same reservoir, fluid, and similar completion and drilling technology, is likely to be interrelated. At the same time, Gong recognized that unconventional reservoirs are statistical plays; two wells with the same drilling and completion designs, drilled 2000-ft apart, could have completely different performances. Because the actual correlation coefficient is unknown, reserves distributions from wells in each sub-area will be summed assuming correlation coefficients of 0 and 1 (arithmetically), since these correlations will bound the correct answer. Last, the aggregation of the P10, P50, and P90 oil and gas estimates between sub-areas will be done arithmetically, per PRMS Guidelines.

4.3. Reserves estimation methodology

In Chapter 2, the oil production BO, VO, and WG sub-areas and gas production DG sub-area were first defined by PVT properties, and then further delimited through thermal maturity, TOC, and formation thickness cut-off values (**Fig. 6**). In Chapter 3, the most appropriate DCA model for each sub-area was found. In this chapter, the minimum decline assumptions, GOR model, and aggregation methodology are presented to complete the reserves estimation methodology. The methodology is summarized below:

1. Select a well from the existing producing wells.

2. Sample from distribution in **Fig. 10 (**a) to get a minimum decline rate for oil wells and **(b)** for gas wells.

3. Apply MCMC DCA (using the most appropriate model determined in the previous chapter) with specific time limit (35 years) and economic limits (1 m^3/day of oil for oil wells in BO, VO, and WG, and 1000 m^3/day of gas for gas wells in WG) [3], as well as sampled minimum decline rate, to forecast production of oil (in BO, VO, and WG) or gas (in DG) on a monthly basis.

4. If the selected well is from the BO, VO, or WG sub-areas, run a MC simulation to sample from **Tables 8 and 9** to get initial GOR and GOR slope and, thus, a monthly GOR forecast.

5. In the same MC simulation, multiply the monthly oil production distribution by monthly GOR to get a monthly gas production forecast distribution.

6. Go back to Step 1 and repeat until all wells have been forecasted.

7. Conduct MC simulations to probabilistically sum individual-well reserves in each sub-area assuming a correlation of 0 between individual-well reserves estimates to get an estimate for full independence between wells.

8. Add individual-well reserve estimates arithmetically (correlation coefficient of 1) to get an estimate for full dependence between wells.

9. Aggregate the estimates across all sub-areas arithmetically to obtain a total estimate of oil and gas reserves for the Vaca Muerta formation.

[3] Personal communication with YPF staff 2017. Buenos Aires, Argentina.

4.4. Results and discussion

The oil reserves estimates from the producing wells in each sub-area as of January 2018, obtained using the methodology described above, are shown in **Tables 11 and 12**. **Fig. 13** shows some of the probabilistic DCA fits of existing wells. Depending on the amount and noise of the historic data of each well, the MCMC simulations resulted in different types of fits; **Fig. 13 (a)** shows examples of wells with better fits, and thus narrower P10/P90 ratios, and **Fig. 13 (b)** shows examples of poorer fits with wider P10/P90 ratios. The estimates for these wells and the resulting P10/P90 ratios are shown in **Table 10**. The individual oil and gas reserves estimates for all wells can be found in Appendix A, while the DCA parameters for the wells in each sub-area are shown in the histograms of Appendix B, together with the correlation plots and coefficients of these variables. Based on the results of the arithmetic aggregation and the probabilistic aggregation using a correlation coefficient of 1, the estimated P90 reserves of oil are between 10.6 and 18.6 MMm^3, the P50 reserves are between 18.4 and 22.2 MMm^3, and the P10 reserves are between 28.5 and 39.5 MMm^3. Similarly, **Tables 13 and 14** show the gas reserves estimates, using the two aggregation methodologies. The total estimated P90 reserves of gas are between 9.4 and 13.6 Bm^3, the P50 reserves are between 27.2 and 33.5 Bm^3, and the P10 reserves are between 74.6 and 62.9 Bm^3.

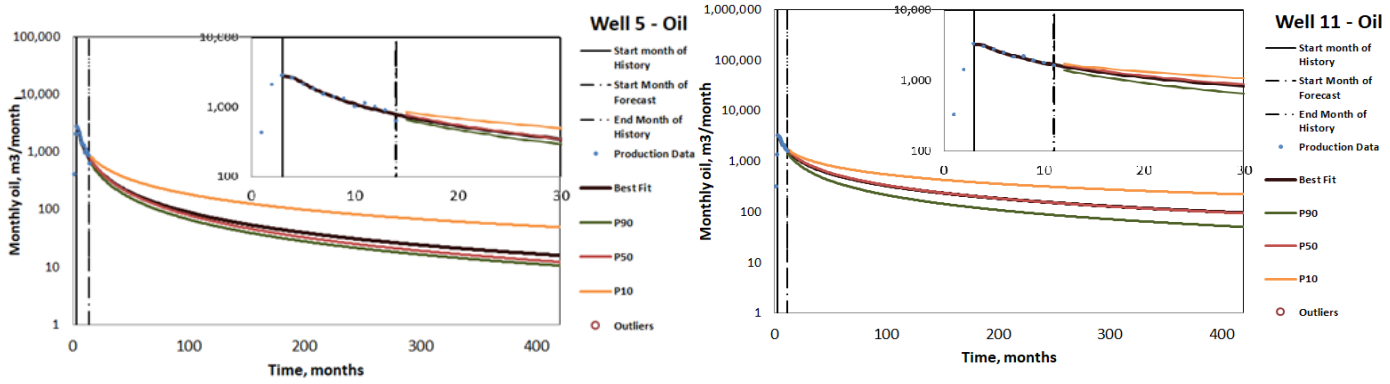

(a)

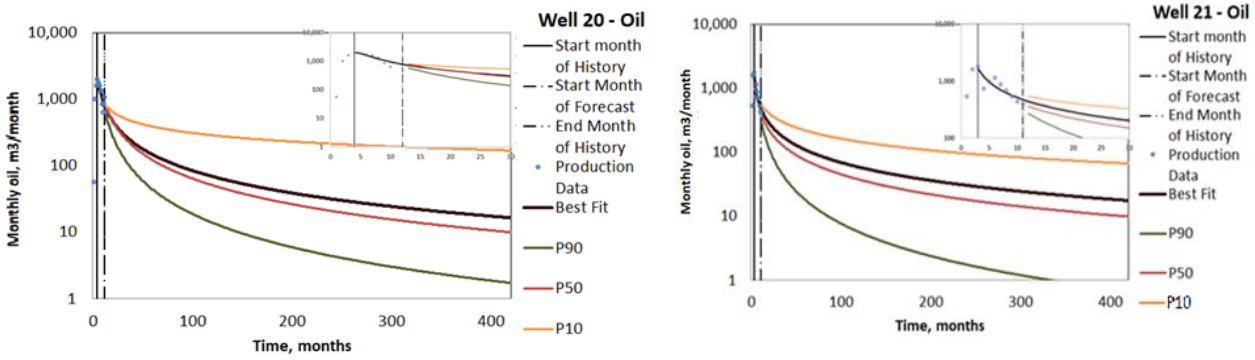

(b)

Fig. 13—Probabilistic DCA examples of wells with (a) good fits and (b) poor fits

Table 10—Probabilistic oil reserves estimates of the example wells as of January 2018, in m^3

Well #	P90	P50	P10	P10/P90
5	12,250	17,282	63,997	5.2
11	24,080	37,407	93,870	3.9
20	3,391	6,702	81,966	24.7
21	11,091	22,733	125,961	11.4

Table 11—Estimated oil reserves for each of the sub-areas as of January 2018, arithmetic aggregation

Sub-area	**# of wells**	**Cumulative oil production, MMm^3**	**Oil reserves**			**P10/P90 ratio**	**P50 EUR per well, MMm^3**
			P90, MMm^3	**P50, MMm^3**	**P10, MMm^3**		
BO	27	1.1	0.7	1.0	2.1	3.0	0.08
VO	104	46.1	7.1	15.5	34.2	4.8	0.6
WG	9	1.4	0.7	1.0	2.1	3.0	0.27
Total	140	48.6	8.5	17.5	38.4	4.5	0.48

Table 12—Estimated oil reserves for each of the sub-areas as of January 2018, probabilistic aggregation using a correlation coefficient of 0

Sub-area	**# of wells**	**Cumulative oil production, MMm^3**	**Oil reserves**			**P10/P90 ratio**	**P50 EUR per well, MMm^3**
			P90, MMm^3	**P50, MMm^3**	**P10, MMm^3**		
BO	27	1.1	0.79	1.1	1.9	2.4	0.08
VO	104	46.1	17.0	20.0	24.7	1.5	0.64
WG	9	1.4	0.78	1.2	1.9	2.4	0.29
Total	140	48.6	18.6	22.2	28.5	1.5	0.51

Table 13—Estimated gas reserves for each of the sub-areas as of January 2018, arithmetic aggregation

Sub-area	# of Wells	Gas reserves			P10/P90 ratio
		P90, MMm^3	P50, MMm^3	P10, MMm^3	
BO	27	98	234	545	5.6
VO	104	5,677	16,793	42,903	7.6
WG	9	2,997	8,476	20,274	6.8
DG	37	778	1,898	11,469	14.7
Total	177	9,452	27,167	74,646	7.9

Table 14—Estimated gas reserves for each of the sub-areas as of January 2018, probabilistic aggregation using a correlation coefficient of 0

Sub-area	# of wells	Gas reserves			P10/P90 ratio
		P90, MMm^3	P50, MMm^3	P10, MMm^3	
BO	27	104	259	523	5.0
VO	104	8,072	21,100	37,508	4.6
WG	9	3,299	9,156	20,247	6.1
DG	37	2,139	3,002	4,617	2.2
Total	177	13,615	33,517	62,895	4.6

When aggregating probabilistically with the correlation coefficient of 0, VO had the narrowest P10/P90 ratio for oil estimates, of 1.5, while DG had the lowest for gas estimates, with a ratio of 2.2. The lower P10/P90 ratios indicate a lower variability in the performance of the wells in these sub-areas, which could be the result of the clustering of most of its wells in the center part of the sub-area. When aggregating arithmetically, WG had the narrowest P10/P90 ratio for oil estimates, of 2.9, with BO as a close second with a ratio of 3. For gas estimates, BO had the lowest, ratio, of 5.6. The larger P10/P90

ratios in gas estimates compared to oil estimates, indicates a higher uncertainty in the fluid type, and the GOR model.

Comparing the overall results using the two aggregation methods, the oil and gas reserves estimates are narrower when aggregating the production of wells in the same sub-area probabilistically, using a correlation coefficient of 0, than when aggregating arithmetically. This is logical since there is a combination of higher and lower reserves estimates when assuming full independence between wells, yielding higher P90 and lower P10 estimates. On the other hand, if wells are fully dependent, as when arithmetically aggregated, wells will be assumed to either be all good or all bad, yielding lower P90 reserves, and higher P10 reserves. Although one aggregation methodology has a lower P10/P90 ratio that the other, both are low for what would be expected for a relatively new area, meaning that uncertainty is being underestimated. For this reason, the arithmetic aggregation method will be used for further discussion.

Based on the results, WG appears as the sub-area with the lowest uncertainty, which is the result of low variability between the few wells in it. As for production, VO has the highest per well oil EUR, with an average of 600 Mm^3, which would make it the most attractive sub-area for oil production for companies willing to take the higher risk, evidenced by the highest P10/P90 ratio out of all sub-areas. The total P90–P50–P10 oil reserves, as of January 2018, using the arithmetic aggregation are 8.5–17.5–38.4 MMm^3.

As for gas production, BO appears to be the sub-area with the lowest uncertainty, which is the result of the low standard deviation of its initial GOR in the GOR model and the low P10/P90 ratio of its oil reserves, compared to the other two oil producing sub-areas. The high P10/P90 ratio of the DG sub-area, that has estimates based on PDCA of real

gas production data, shows the GOR model could be underestimating uncertainties, and/or that gas wells have more uncertainty in their production than oil wells and their associated gas production. The total P90–P50–P10 gas reserves, as of January 2018, using the arithmetic aggregation are 9.5–27.2–74.6 Bm^3.

5. CONTINGENT AND PROSPECTIVE RESOURCES

Recalling the definition from the first chapter, contingent resources refer to "those quantities of petroleum estimated, as of a given date, to be potentially recoverable from known accumulations, but the applied project(s) are not yet considered mature enough for commercial development due to one or more contingencies" (PRMS 2011). Future wells drilled within a certain distance away from existing wells would be considered to be targeting known accumulations. Since it is not public information which wells will be drilled in the next five years to comply with the definition of reserves, the volumes of oil and gas produced from these future wells will be classified as contingent resources. Prospective resources are "those quantities of petroleum estimated, as of a given date, to be potentially recoverable from undiscovered accumulations by application of future development projects" (PRMS 2011). Given these definitions, the difference between contingent and prospective resources lies in the discovery of the accumulations. Known or discovered accumulations need "one or several exploratory wells [to] have established through testing, sampling, and/or logging the existence of a significant quantity of potentially moveable hydrocarbons" (PRMS 2011). It is not clear in the PRMS guidelines how far away from existing wells one can say there are known accumulations. Given the large heterogeneities in the Vaca Muerta shale play, for this study, the property of being discovered will be extrapolated to one section (640 acres) around existing wells, as shown in **Fig. 14** for vertical (a) and horizontal wells (b), assuming existing horizontal wells have 2000 m long laterals, since the actual horizontal length is not public information. **Fig. 14** (c) shows an example of how 2000 m long wells would fit within one section of an existing well, with a spacing of 350 m between them which allows for

only two other wells to fit in the one-section area. The number of wells that would fit within one section of existing wells will depend on well-spacing and the proximity of existing wells that could result in an overlap of the one-section areas. **Fig. 16** shows all the one section areas around existing wells with known accumulations in blue and the undiscovered areas in grey. **Table 15** summarizes the areas for prospective and contingent resources. The areas in this table do not subtract out the areas associated with reserves of existing wells. The way the areas of the existing wells were accounted for will be explained later in this chapter after explaining the well-spacing assumptions and resource classification criteria.

The estimated oil and gas volumes from wells that would be drilled within one section away from existing wells will be defined as contingent resources. The estimated oil and gas volumes from wells that would be drilled more than one section away from existing wells will be defined as prospective resources. Given the better economic results of horizontal wells (over vertical wells), and current trend of all companies to drill only horizontal wells for production,[4] all future wells will be assumed to be horizontal. Possible interference between wells was not taken into account because there is no historical data on which to base the reduction of EUR from interference.

[4] A few vertical wells are still drilled for geologic study purposes. Some of these wells are later turned into producers through the drilling of sidetracks or hydraulic stimulation of the vertical section going through the Vaca Muerta formation.

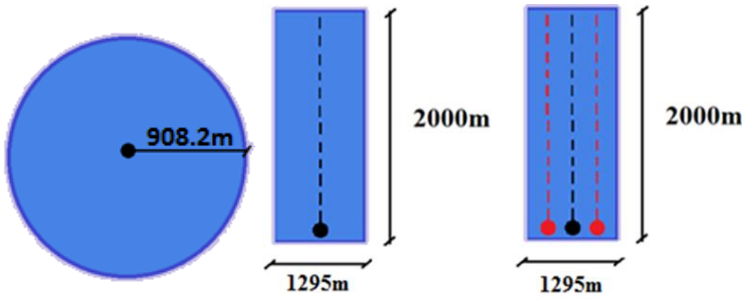

(a) (b) (c)

Fig. 14—(a) One section (blue) around an existing vertical well (black) (b) one section (blue) around an existing 2000 m long well (black), considered discovered. (c) In red, wells that would fit within one section around an existing well, with 2000m long lateral lengths

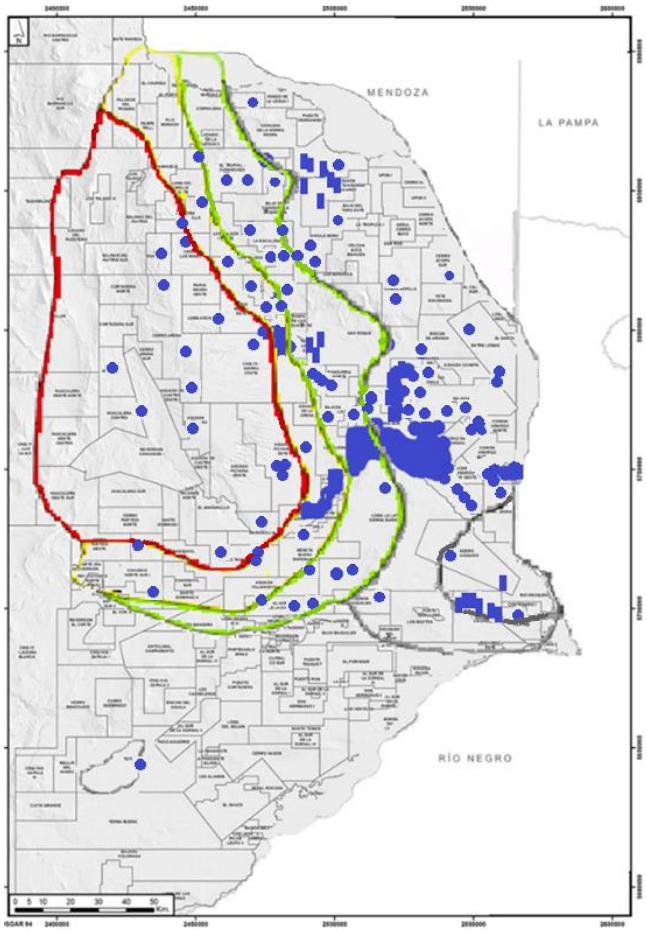

Fig. 15—Discovered (blue) and undiscovered (grey) accumulations

Table 15—Resources areas per sub-area

Sub-area	Contingent resources area, km^2 (Blue)	Prospective resources area, km^2 (Grey)
BO	156	7,878
VO	71	3,170
WG	52	2,118
DG	41	7,506

5.1. Generation of probabilistic type decline-curves for each of the four sub-areas: BO, VO, WG, and DG

Production from existing wells were used to create a type decline-curve for each of the sub-areas. The type-decline curves were used to estimate the oil and gas resources by combining them with the well-spacing assumptions that will be described later in this chapter, and the drilling efficiency. The same 223 horizontal wells used to estimate reserves of the previous chapter were used to create the type-decline curves. As can be seen in **Fig. 7**, most wells are located in the center of the VO and BO sub-areas towards the border between them, and in the eastern part of the DG sub-area, with exploratory wells in most of the concession blocks (dispersed throughout the map). The clustering of existing wells, combined with the heterogeneities throughout the Vaca Muerta formation, will be reflected in a higher uncertainty in the results, as the available data from the remaining parts of the formation is limited. With the limited number of wells in the dataset, the uncertainty in finding the representative type-decline curve for the entire area is larger than if more wells were available. This uncertainty is in addition to the

uncertainty in the production profile from any well or group of wells, and was not accounted for in this thesis. The type decline-curves for each sub-area will show the distributions of oil (for BO, VO, and WG) and gas (for DG) of new wells, assuming drilling and completion designs similar to the wells used in the construction of the type decline-curves.

The following methodology to generate the type-decline curves for each sub-area from Gong et al (2014) was followed:

1. Perform a probabilistic decline-curve forecast with MCMC simulations of the selected wells, using the model with the best fit for each sub-area determined in Chapter 3, and all the production data available for each well.
2. Record the decline-curve parameters for all wells in each sub-area.
3. Perform a Monte Carlo simulation to randomly draw 100,000 parameter sets of all decline-curve parameters for each sub-area, a minimum decline rate, an initial GOR and a GOR slope. The decline-curve parameters were drawn together as a set (dependent on each other), the initial GOR was drawn from the lognormal distribution described in **Table 9**, and the GOR slope was drawn from the uniform distributions with boundaries in **Table 8**.
4. Use each set of variables to create a decline curve of oil (for BO, VO, and WG) or gas (for DG), and estimate the associated monthly gas in the oil sub-areas.
5. Use the monthly oil/gas values to create a distribution for each month.

6. Use the P10, P50, and P90 monthly values from the distributions to create the P10, P50, and P90 oil (in BO, VO, and WG) and gas (in DG) type-decline curves from the distribution.

7. Use the distribution of the associated gas calculated in step 3 to find the P10, P50, and P90 gas in the oil regions.

Figs. 16, 17, 18 and 19 show the type decline-curves for the four sub-areas. **Table 16** summarizes the oil and gas technically recoverable resources at 35 years (TRR35) of the P10, P50, and P90 type curves in each sub-area.

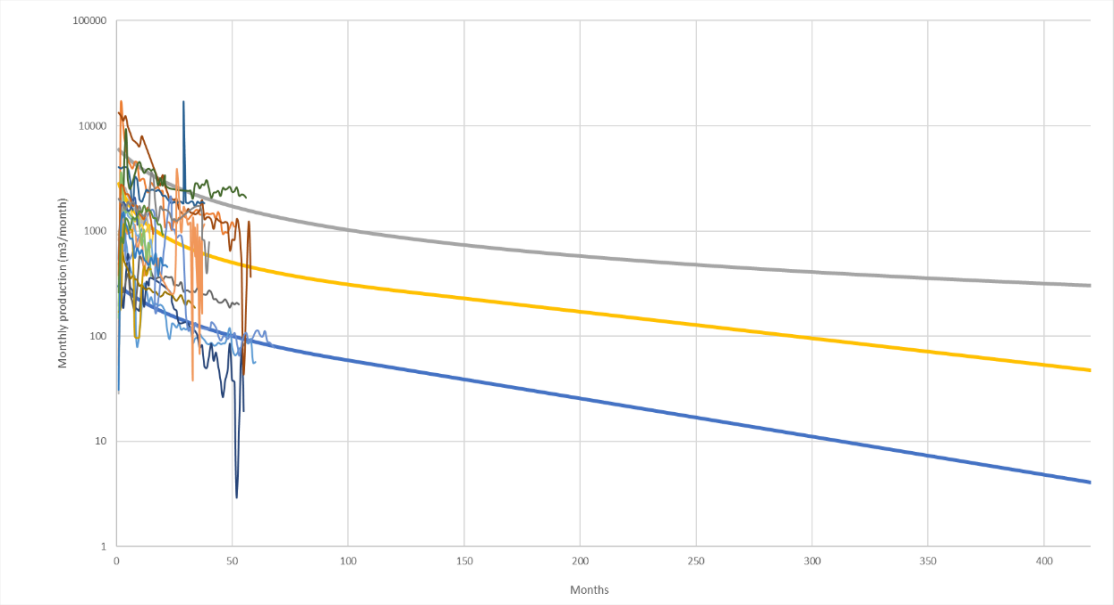

Fig. 16—Oil production P90–P50–P10 type decline-curves for the BO sub-area

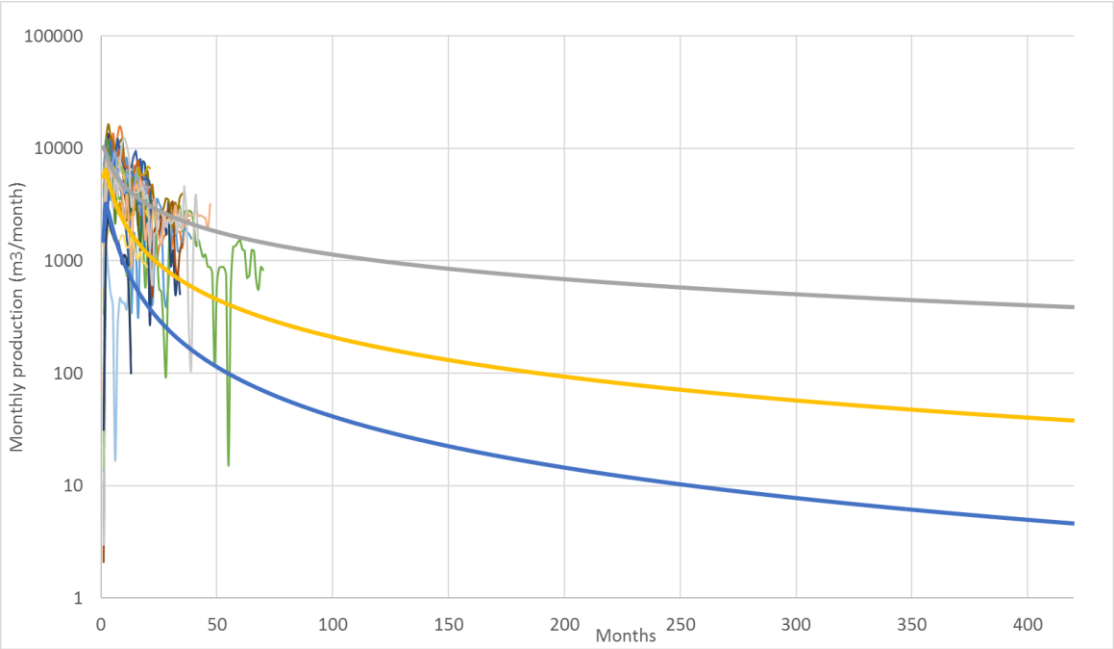

Fig. 17—Oil production P90–P50–P10 type decline-curves for the VO sub-area

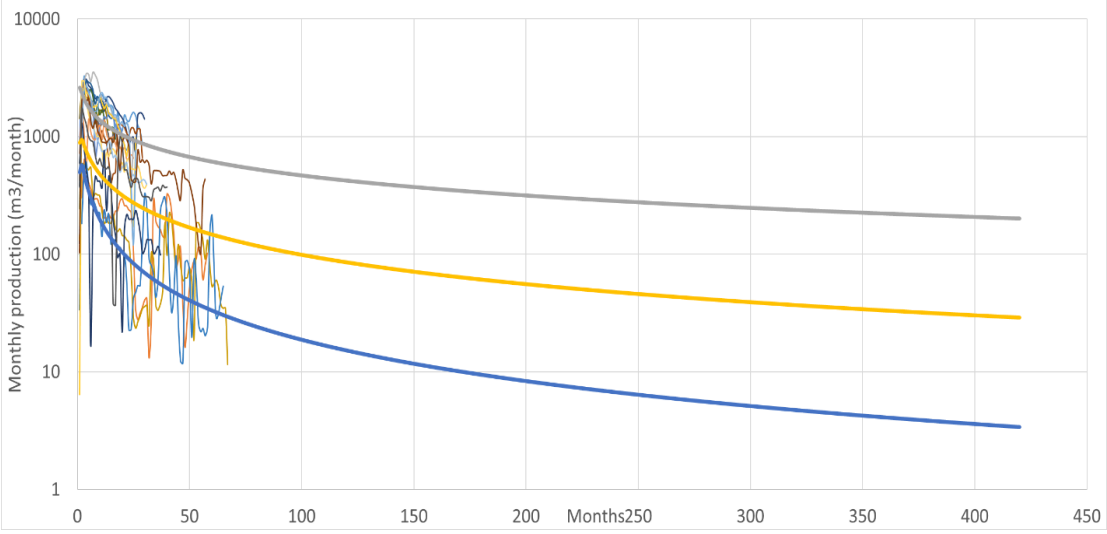

Fig. 18—Condensate production P90–P50–P10 type decline-curves for the WG sub-area

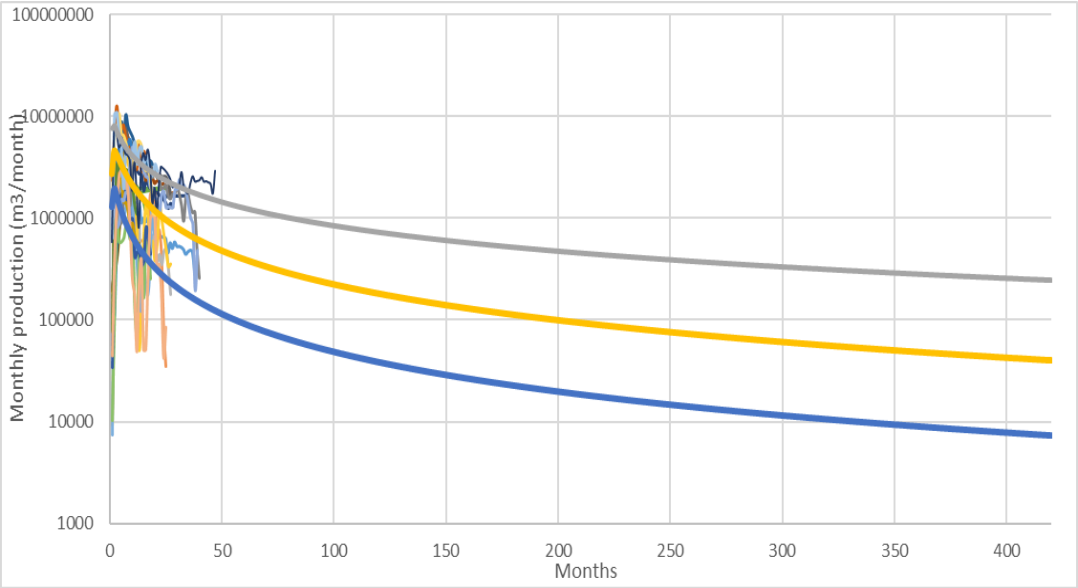

Fig. 19—Gas production P90–P50–P10 type decline-curves for the DG sub-area

Table 16—Summary of oil and gas TRR35 per well in each sub-area

Production Sub-areas	Oil TRR35, Mm3					Gas TRR35, MMm3				
	P90	P50	P10	Mean	P10/P90	P90	P50	P10	Mean	P10/P90
BO	19	116	403	179	21	2.3	12	39	18	17
VO	17	83	329	197	20	6.5	31	123	53	19
WG	3.9	26	79	39	20	2.4	44	130	61	54
DG						37	215	459	276	12

5.2. Well-spacing assumptions

Well-spacing in Vaca Muerta evolved over the last 6 years, increasing spacing to avoid fracture hits in regions with natural fractures and faults, while not leaving unproduced reservoir volumes in between wells. Currently, the well-spacing ranges between 200–400 m (656–1,312 ft) for the BO, VO, and WG sub-areas. For the DG sub-area this range

is between 900–1,100 m (2,952–3,608 ft). These ranges depend on fracture growth and the formation thickness, since in a thicker part of the formation, wells can go to different depths, allowing them to be drilled closer together horizontally. Lateral lengths of new wells currently range between 2000–3200 m (6,562–10,499 ft). Combining the ranges of current well-spacings and lateral lengths yields a range of 99–316 acres/well in the BO, VO, and WG sub-areas, and 445–870 acres/well in the DG sub-area. Well-spacing will then be modeled with uniform distributions using these ranges: 99–316 acres/well for BO, VO, and WG, and 445–870 acres/well for DG (**Table 17**).

Since the spacing between wells is variable and the drilling surveys of existing wells is not public information (only the wellhead´s coordinates are), to account for the area of the existing wells associated with reserves, one could not just subtract a fixed area from the contingent resources area. To solve this, after calculating the number of wells that would fit in the contingent resources area probabilistically, for each sub-area, the number of existing wells was subtracted from them. While this is not the most precise methodology, it is the best that can be done with the available data.

As previously mentioned, the Vaca Muerta formation spans over a large areal extension. It underlays mountains, cities, and native communities. This means there are regions that are not drillable for hydrocarbon production. Furthermore, there are geological properties in some regions that make drilling and stimulating wells difficult, like faults, and inverse stresses. While faults cause a poor fracture propagation due to channelization, inverse stresses are avoided because they make fractures grow horizontally. Last, concession blocks are very irregular-shaped, reducing the drilling efficiency even further (**Fig. 15**). For these reasons, a drilling efficiency factor was used by well of each well. Because at

this point of the development not all the areas with the geological properties that would make drilling and stimulating difficult have been identified, and measuring exactly the lost area to irregular-shaped blocks, mountains, and cities with their growth rate, would be a difficult task, the drilling efficiency factor was modeled as a random variable uniformly distributed between 1 and 1.4 (**Table 17**). The higher end of this distribution is based on the maximum area estimated to not be utilized due to irregular shape, 25% as assumed by Gong (2013), and an arbitrary factor of 0.95 multiplied times the remaining 75% of the area to account for the remaining variables that could reduce the drillable areas, mentioned above, to obtain 71.25%. Given the way the drilling efficiency factor is incorporated into the model (by multiplying it times the acreage per well), the 71.25% was inverted to obtain the 1.4 of the higher end of the uniform distribution of the drilling efficiency factor.

Table 17—Summary of the minimum and maximum values of the uniform distributions described in this section

Assumption	Minimum	Maximum
Acreage per well in oil sub-areas (BO, VO, and WG)	99	316
Acreage per well in gas sub-area (DG)	445	870
Drilling efficiency factor	1	1.4

5.3. Economic evaluation

For the resources estimates to eventually become reserves, one of the multiple criteria they need to pass is a commercial criterion. If the type-wells prove to be commercial through an economic evaluation, the chances are higher that future wells projected in this study will be drilled, giving more significance to the resources estimations presented in this thesis.

Currently, in Argentina, to incentivize the development of unconventional plays, prices of "unconventional gas" are ruled by Resolution 419/17 (Pourteau 2017). Resolution 419/17, better known as "Plan Gas", defines "unconventional gas" as the:

> …gas coming from a reservoir characterized by very compacted sandstones or shales with low porosity and permeability which would impede natural migration of fluid and would therefore require use of advanced technologies for its commercial production (…) The subsidy will only be given to concessions in the Neuquén basin with a specific investment plan for this subsidy program (…) Initial production must be less than 500,000 m^3 per day…

Gas production falling within this classification would receive the following benefit: "The minimum price will be 7.50 USD/MMBTU for 2018, 7.00 USD/MMBTU for 2019, 6.50 USD/MMBTU for 2020, 6.00 USD/MMBTU 2021." If no extensions are made to this law, prices will resume to be ruled by international gas prices after 2021.

The main assumptions for the economic evaluation are shown in **Table 18**. Estimates of costs, royalties, and taxes were obtained from YPF's presentation for investors (YPF S.A. 2017). The oil and gas economic limits were obtained from personal communication with YPF staff (2017). A gas shrinkage factor of 10% was assumed to account for gas losses in the separation process and flaring. For simplicity, the economic evaluation was done deterministically, assuming a lower oil price than the current WTI $57/barrel, and gas

price of $3/MMBTU, which is about the current Henry Hub price. The removal of the gas subsidies was assumed, in case the Plan Gas is removed and to make the analysis valid for wells drilled after 2021. An average type decline-curve for each sub-area was used, calculated using Swanson's rule, by summing 0.3 times the P90, 0.4 times the P50, and 0.3 times the P10 oil/gas production curves.

Table 18—Economic assumptions to determine offset wells resource classification

Assumptions	
Drilling and completion costs, $MM	4.8
Tie-in costs, $MM	3
Variable operating cost, $/MBoe	0.6
Gas price, $/MMBTU	3
Oil price, $/bbl	50
Ad valorem taxes	3.5%
Federal income tax	35%
Royalties	22%
Oil economic limit (m^3/day)	1
Gas economic limit (m^3/day)	1000
Gas shrinkage factor	10%

The economic analysis using the assumptions listed above yield the results in **Table 19**. Although these results will be discussed in detail in the following section, it is important to point out that the DG sub-area is not economic under the current Henry Hub gas price assumption of $3/MMBTU.

Table 19—Economic evaluation results of future wells

Sub-area	NPV10, $MM	IRR	Payout, months
BO	5.62	29.3%	32
VO	18.05	42.3%	19
WG	9.90	28.2%	37
DG	-3.37	-1.4%	-

Given the sub-economic results of the DG sub-area, its average type-decline curve was then evaluated under the Plan Gas prices, assuming it would be put into production in January 2018, to evaluate it under the current condition. The results of the economic evaluation of the DG sub-area under Plan Gas prices are shown in **Table 20**.

Table 20—Economic evaluation results of the DG sub-area under Plan Gas price assumptions

Sub-area	NPV10, $M	IRR	Payout, months
DG	965.5	16.1%	40

This analysis shows the importance of the Plan Gas for incentivizing the development of the gas resources of the Vaca Muerta formation. Keeping all other variables constant, after 2021, or if Plan Gas is removed, gas prices would have to be $5.15/MMBTU, or drilling and completion costs would have to decrease to $4.4 million, for DG wells to break even. I assume Plan Gas will not be removed and will remain in place through 2021 in my estimation of gas resources in the following sections. By the end of the Plan Gas in 2021, companies wanting to produce from the DG sub-area will have to find ways to reduce costs, or increase production from wells and maintaining current costs, to make wells in this sub-area commercial.

5.4. Resources estimation methodology

In previous sections in this chapter, I explained how the resources areas were estimated, the probabilistic type decline-curves for each sub-area were created, and the well-spacing assumptions and drilling efficiency factor were determined. The methodology used to integrate all these variables to estimate oil and gas resources is summarized below:

1. Take the total resource area for one sub-area and resource classification from **Table 15**. Perform a MC simulation to:
    a. Multiply the acreage per well of the selected sub-area/resources times the drilling efficiency (from **Table 17**), divide the sub-area/resources area by this result, and subtract the number of existing wells (**Table 7**) from the sub-area to obtain the distribution of the number of wells for the sub-area/resources combination.
    b. Multiply the distribution of the number of wells from Step 1.a. by the oil type-decline curve (for the BO, VO, and WG sub-areas) or gas type-decline curve

(for the DG sub-area) to obtain the oil or gas production forecast for the selected sub-area and resource classification.[5]

c. If estimating the resources of the BO, VO, or WG sub-areas, sample from **Tables 8** and **9** to get initial GOR and GOR slope, respectively, and from this a monthly GOR forecast.

d. Multiply monthly oil production by monthly GOR to get a monthly gas production forecast.

2. Repeat Steps 1.a.–1.d. for all sub-areas and resource classifications.

3. Aggregate the estimates across all sub-areas for each resources classification arithmetically to obtain estimates of total oil and gas contingent and prospective resources for the Vaca Muerta formation.

5.5. Results and discussion

The positive NPV10 of the type-wells in the BO, VO, and WG sub-areas obtained from the economic evaluation (**Table 16**) shows their commerciality. The commerciality calculation, and thus the resources estimates, for the BO, VO, and WG sub-areas assume that future wells in these sub-areas will be drilled under a slightly lower oil price[6] and current drilling and completion costs scenario. The sub-economic results of the DG sub-area under the current Henry Hub gas price and current drilling and completion costs assumptions show that costs will have to decrease if companies want to exploit this sub-area after the Plan Gas ends in 2021. Interpreting the results the other way around, they

[5] Using this methodology adds individual-well oil and gas resource estimates arithmetically, following the methodology used in Section 4.3, to get a distribution for oil and gas resources for each sub-area.
[6] Of $50/barrel, compared with the current $57/barrel of the WTI.

show the importance of the Plan Gas subsidy for the Argentine government to reach the goal of recovering the energy self-sufficiency in the short run.

Table 21 shows the volumes from new wells that would be drilled within one section of the existing wells, as of January 2018, classified as contingent resources. **Table 22** shows the volumes from new wells that would be drilled one section away from existing wells, as of January 2018, classified as prospective resources.

Table 21—Contingent resources for the Vaca Muerta formation by sub-area, as of January 2018

		Oil, MMm^3				Gas, Bm^3			
Production Sub-areas	Mean # of wells	P90	P50	P10	P10/P90 ratio	P90	P50	P10	P10/P90 ratio
BO	312	6.0	36.2	126.1	21	0.72	3.6	12.3	17
VO	142	2.3	11.7	46.8	20	0.92	4.3	17.5	19
WG	104	0.41	2.7	8.2	20	0.25	4.6	13.5	54
DG	18					0.69	3.9	8.3	12
Total	558	8.8	50.6	181.1	21	2.6	16.4	51.5	20

Table 22—Prospective resources for the Vaca Muerta formation by sub-area, as of January 2018

		Oil, MMm^3				Gas, Bm^3			
Production Sub-areas	Mean # of wells	P90	P50	P10	P10/P90 ratio	P90	P50	P10	P10/P90 ratio
BO	15,756	299	1,828	6,350	21	36	181	621	17
VO	6,339	108	526	2,086	19	41	193	781	19
WG	4,236	17	110	335	20	10	188	550	54
DG	3,336					123	717	1,531	12
Total	26,331	424	2,464	8,771	21	211	1,279	3,483	17

According to the results shown in the tables above, BO has the highest contingent and prospective oil resources and the highest P10/P90 ratio. The slightly lower P10/P90 ratio in VO compared to the other sub-areas could result from the lower uncertainty coming from having more information from the larger number of wells already producing. DG has the highest gas resources, and the lowest P10/P90 ratio. The P10/P90 ratios in the gas estimates of the oil-producing sub-areas are linked to the oil P10/P90 ratios, as well as the uncertainty in the GOR model for each sub-area. Sub-area WG had the highest standard deviation in the initial GOR and the widest range for the GOR slope. The total gas estimates in both resources estimations show a lower P10/P90 ratio than the oil P10/P90 ratios, indicating that the simulation methodology used to combine oil production and GOR model may be underestimating uncertainty. The oil and gas resources estimates in Tables 20 and 21 show higher P10/P90 ratios (19 to 21 for oil and 12 to 54 for gas) than the P10/90 ratios of the oil and gas reserves estimates in Tables 10 and 12 (3 to 4.8 for oil and 5.6 to 14.7 for gas). The higher P10/P90 ratios in the resources estimates show the higher uncertainty in future, undrilled wells. Since the same methodology was used for both contingent and prospective resources calculations, and arithmetic aggregation was used, their P10/P90 ratios are very similar.

6. COMBINED RESULTS

The estimated oil and gas volumes of the contingent and prospective resources estimates were added arithmetically, together with the reserves estimates, to obtain TRR estimates to compare with estimates from previous studies mentioned in **Table 1**. Given the relatively small cumulative production from older wells, compared to the magnitude of the estimated resources, the combined TRR estimated from this thesis can still be compared to the TRR estimates from older studies. The combined results for reserves, contingent resources, and prospective resources are shown in **Table 23**. Adding up the volumes in all three classifications allows a comparison with previous estimates in **Table 24** and **Figs. 20** and **21**. Based on the comparison, the following can be concluded:

- The probabilistic estimates in this thesis account for the uncertainties in well-spacing, well-length, GOR and GOR evolution over time, oil and gas production, time to BDF, and minimum decline rate once wells reach BDF.
- The P10/P90 ratio of the oil TRR estimate, 21.27, is wider than the 2.02 ratio of the only other probabilistic study by Gutierrez Schmidt et al. (2014). The higher ratio is likely a more realistic estimate of the actual uncertainty, compared to the probabilistic volumetric analysis by Gutierrez Schmidt et al.
- Oil estimates of older studies fall within the range of the estimates provided in this thesis. At the same time, the P50 estimates of this thesis are less than half the study by Gutierrez Schmidt et al. (2014), and slightly less than the latest EIA estimate from 2015.
- The gas estimates from this thesis are significantly lower than those from the deterministic volumetric studies by the EIA (2011 & 2015) and Barredo & Stinco

(2014). This is possibly because the recovery factor used in the volumetric studies by the EIA, 35% of the in-place volumes, could be high in comparison to the actual recoveries from the wells with current drilling and completion designs.

- The overall gas TRR P10 from this thesis is slightly higher (8.5%) than the P10 estimate from YPF (2011). As the major company exploiting the Vaca Muerta formation, YPF has more subsurface data available (e.g., geological, petrophysical, geophysical) to better assess the potential of the formation. On the other hand, the YPF study is also dated, so the difference could result from less production data being available from vertical wells.
- This thesis is the first probabilistic study to provide the full P90–P50–P10 distribution of estimated oil and gas TRR and to publish the methodology used.
- This thesis is the first public study conducted using probabilistic DCA and actual production data, which should make it more reliable than estimates from older studies conducted using analogies with US plays and volumetric estimates.

Table 23—Combined results (reserves, contingent resources and prospective resources, as of January 2018) of this thesis

		Oil TRR35, MMm^3				Gas TRR35, Bm^3			
Production Sub-areas	Mean # of wells	P90	P50	P10	P10/P90 ratio	P90	P50	P10	P10/P90 ratio
BO	15,756	306	1865	6478	21	37	185	634	17
VO	6,339	120	554	2168	18	48	214	841	18
WG	4,236	18	114	345	19	13	201	584	44
DG	3,336					124	723	1551	12
Total	26,331	443	2533	8992	20	223	1323	3609	16
		Oil TRR35, Bbbl				Gas TRR35, Tcf			
Total	26,331	2.78	15.93	56.55	20	7.88	46.71	127.45	16

Table 24—Comparison between previous estimates, and the estimates of this theses

Author(s)	Type of classification	Oil, Bbbl				Gas, Tscf				Method
		Mean	P10	P50	P90	Mean	P10	P50	P90	
EIA (2011)	Technically recoverable resources	-	-	-	-	240.00	-	-	-	Analogs and volumetric method
YPF (2011)	Technically recoverable resources	-	40.00	-	-	-	117.00	-	-	Not specified
Gutierrez Schmidt et al. (2014)	Prospective resources	36.70	55.40	39.50	27.40	-	-	-	-	Probabilistic volumetric method
Stinco & Barredo (2014)	Technically recoverable resources	-	-	-	-	220.00	-	-	-	Volumetric method
EIA (2015)	Technically recoverable resources	16.20	-	-	-	307.70	-	-	-	Analogs and volumetric method
This thesis (2019)	Reserves	-	0.24	0.11	0.05	-	2.64	0.96	0.33	Probabilistic DCA
	Contingent resources	-	1.14	0.32	0.06	-	1.82	0.58	0.09	
	Prospective resources	-	55.17	15.50	2.67	-	123.00	45.17	7.45	
	Technically recoverable resources	-	56.55	15.93	2.78	-	127.45	46.71	7.88	

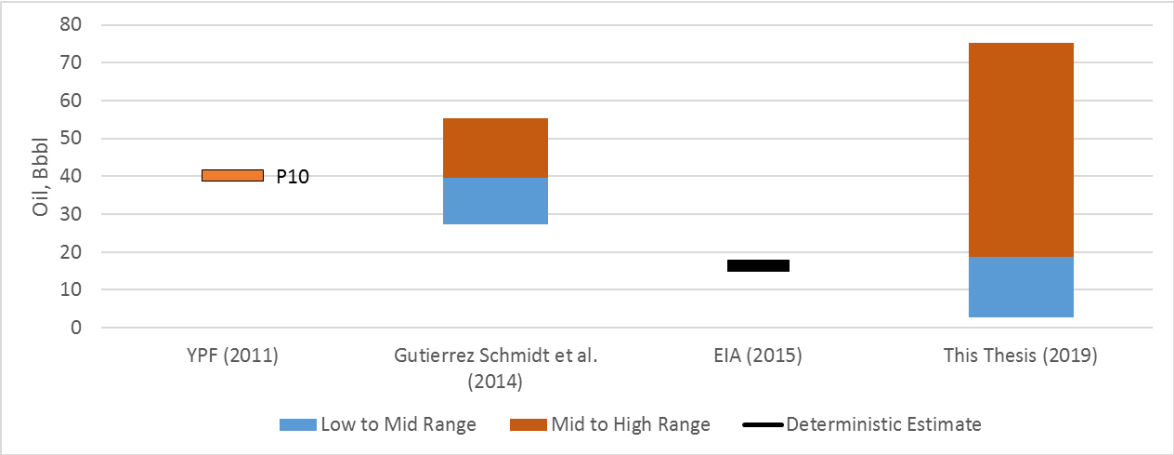

Fig. 20—Comparison of oil estimations

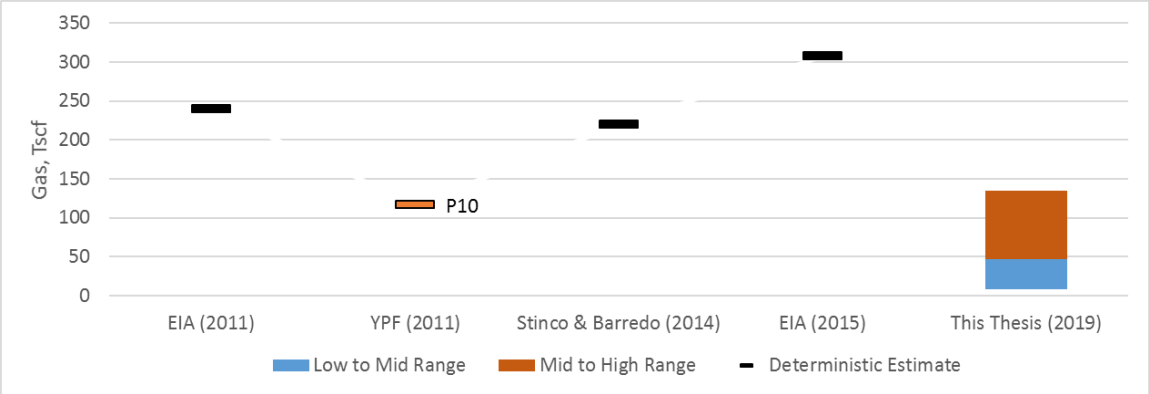

Fig. 21—Comparison of gas estimations

7. CONCLUSIONS

Based on the study of the Vaca Muerta formation, in the Neuquén Basin, Argentina, presented in this thesis, the following can be concluded:

- As of January 2018, estimated P90–P50–P10 reserves associated with existing wells are 8.5–17.5–38.4 $MMm^3$of oil, and 9.5–27.2–74.6 Bm^3 of gas.
- As of January 2018, the estimated P90–P50–P10 contingent resources corresponding to wells within one section (640 acres) of existing wells are 8.8–50.6–181.1 MMm^3 of oil, and 2.6–16.4–51.5 Bm^3 of gas.
- As of January 2018, the estimated P90–P50–P10 prospective resources are 424–2,464–8,771 MMm^3 of oil and 211–1,279–3,483 Bm^3 of gas.
- This is the first public update of the reserves and resources estimates using actual production data from wells with new designs, and the lower drilling costs published by YPF.
- While oil TRR estimates in this thesis provide a wider range of results compared to older studies and bracket the results from older studies, gas estimates are lower than previous estimates done with volumetric methodologies or through analogy with US plays.
- The P10/P90 ratio of oil and gas TRR estimates, of 20 and 16 respectively, are what would be expected for a new development like this. Conversely, the low P10/P90

ratios in the reserves estimations, between 3 and 3.9, indicate that some uncertainties are likely being underestimated.

7.1. Future Work

As described by Emmanuel d'Huteau (2017) in his lectures, the Vaca Muerta (Dead Cow) formation, is not just one cow, but a herd of cows due to the heterogeneities throughout its large areal extension. As new exploratory wells are drilled in sub-areas WG and DG, this study should be updated to contemplate possible differences with the few wells available today, that were used in the construction of type-decline curves for this study and identifying the most appropriate DCA model in each sub-area. Furthermore, the four sub-areas studied (BO, VO, WG, and DG) could be further subdivided, given their large areal extensions, to obtain better results, as more information becomes available from new wells. Another limitation of the methodology adopted is the assumption that wells will have an optimal spacing and will not interfere with each other, given the lack of historical data and public records of well interferences. As interferences become more common and we have more information on their effects on the EUR, they could be incorporated to the model. Finally, as mentioned in Section 5.5, using a single sampled GOR forecast (as opposed to the distribution of GOR forecasts) per oil forecast in the Monte Carlo process may underestimate the uncertainty of gas TRR estimates. A more rigorous model that combines the uncertainty in the GOR forecasts with the uncertainty in the oil forecasts may better assess the uncertainty in the gas TRR estimates.

NOMENCLATURE

a	Is the is the intercept of the straight line of the log-log plot of q/G_p vs t for gas, or q/N_p vs t for oil
b	Arps hyperbolic decline constant
Bbbl	Billion barrels of oil
Bm^3	Billion cubic meters
BDF	Boundary-dominated flow
BO	Black-oil sub-area
Bscf	Billion standard cubic feet
d_i	The initial nominal decline rate in the Arps model, in 1/month [1/time]
D_1	Decline constant intercept at 1 month, *D(t=1 month)* in the power-law model
D_∞	Decline constant at "infinite time", *D(t=∞)*, in the power-law model
$\widehat{D}_t$	Decline constant defined by the D-parameter equation, $\widehat{D}_t = D_1/n$, in the power-law model
DCA	Decline-curve analysis
DG	Dry-gas sub area
EIA	Energy Information Administration
ENE	East-northeast
EUR	Estimated ultimate recovery
GOR	Gas/oil ratio
IRR	Internal rate of return
$-m$	Is the negative slope of the straight line of the log-log plot of q/G_p vs t for gas, or q/N_p vs t for oil, in the Duong model

MBoe	Thousand barrels of oil equivalent
MCMC	Markov Chain Monte Carlo
MMBTU	Million British thermal units
MMbbl	Million barrels of oil
Mm^3	Thousand cubic meters
MMm^3	Million cubic meters
n	Exponent parameter for SEPD and power-law models
NNW	North-northwest
NNE	North-northeast
NPV10	Net present value at a 10% discount rate
OOIP	Original oil in place
OGIP	Original gas in place
PDCA	Probabilistic-decline-curve analysis
PDTSP	Production during the second period
PRMS	Petroleum Resource Management System
P10	Value at confidence interval 10%
P50	Value at confidence interval 50%
P90	Value at confidence interval 90%
q_1	Flow rate at day 1 used in the Duong model, in m^3/day [vol/time]
q_i	The initial production rate, in m^3/month [vol/time]
q_∞	Rate at infinite time, in m^3/day [vol/time]
Ro	Vitrinite reflectance
scf	Standard cubic feet
SD	Standard deviation

SEC	Securities and Exchange Commission
t	Cumulative time since start of production, in months [time]
τ	Characteristic time parameter for SEPD model, in months [time]
TOC	Total organic content
TRR35	Technical recoverable resources of 35 years
Tscf	Trillion standard cubic feet
USD	United States Dollar
VO	Volatile-oil sub-area
WG	Wet-gas and condensate sub-area
$MM	Million dollars

REFERENCES

Ali, T. A., Sheng, J. J. 2015. Production Decline Models: A Comparison Study. Proc., SPE Eastern Regional Meeting, Morgantowwn, West Virginia, USA.

Argentina Shale. 2017. *Inversiones En Vaca Muerta Sumarían u$s10.000 Millones En 2018*: Argentina Shale (Reprint). www.argentinashale.com/exploracion-y-desarrollo/inversiones-en-vaca-muerta-sumarian-us10-000-millones-en-2018/.

Arps, J. J. 1945. Analysis of Decline-curves (in English). *Transactions of the American Institute of Mining and Metallurgical Engineers* **160**: 228-247. //WOS:A1945XR32700018.

Askenazi, A., Biscayart, P.,Caneva, M. et al. 2013. Analogia entre la Formacion Vaca Muerta y Shale Gas/Oil Plays de EEUU. *Society of Petroleum Engineers* **Argentine Section, Young Professionals Committee**. JJPP0003.

Barredo, S.P., Cristallini, E., Zambrano, O. et al. Geodinámica de las cuencas sedimentarias. *Mar del Plata, Argentina*, 443-446: Instituto Argentino del Petróleo y del Gas.

Barredo, S.P., Stinco, L.P. 2014. Unconventional Reservoir Geology of the Neuquén Basin Argentina. Proc., SPE Anual Technical Conference and Exhibition, Amsterdam, The Netherlands.

Boulis, A., Ramkumar Jayakumar, F. L. et al. 2013. Improved Methodologies for More Accurate Shale Gas Assessments. Proc., SPE Americas Unconventional Resources Conference.

Buck, W.R. 1991. Mode of continental lithospheric extension. *Journal of Geophysical Research* **96**: 20161-20178.

Capen, E. C. 2013. The Difficulty of Assessing Uncertainty (includes associated papers 6422 and 6423 and 6424 and 6425). *Journal of Petroleum Technology* **28** (08): 843-850.

Caraballo, I. E., Sacchetta, F.A, Acosta, M. 2016. "Vaca muerta y el sueño del autoabastecimiento." *El Economista*, December 27.

Cruz, C.E., Robles, F., Sylwan, C.A.et al. Los sistemas petroleros jurasicos de la Dorsal de Huincul. Cuenca Neuquina. Argentina. *Buenos Aires*, 175-195: Instituto Argentino del Petroleo y el Gas.

d'Huteau, E. 2017. *Fracturas Hidraulicas*. Añelo, Neuquén, YPF.

Duong, A. N. 2013. Rate-Decline Analysis for Fracture-Dominated Shale Reservoirs. *SPE Reservoir Evaluation & Engineering* **14** (03): 377-387.

EIA. 2011. *World Shale Gas Resources: An Initial Assessment of 14 Regions Outside the United States*. Washington DC, U.S. Energy Information Administration (Reprint).

EIA. 2015. *World Shale Gas Resources: An Initial Assessment of 14 Regions Outside the United States*. Washington DC, U.S. Energy Infromation Agency (Reprint).

Fernandez Seveso, F., Tankard, A.J. 1995. Tectonics and stratigraphy of the late Paleozoic Paganzo Basin of western Argentina and its regiona implications. In *Petroleum basins of South America*, ed. A.J. Tankard, R. Suarez Soruco and H.J. Welsink, 285-301. Tulsa, American Association of Petroleum Geologists.

Freeborn, R., Russell, B. 2016. Creating More-Representative Type Wells. *SPE Economics & Management* **8** (02): 50-58.

Gas y Petroleo del Neuquén. 2018. Vaca Muerta, http://www.gypnqn.com.ar/vacamuerta.html (downloaded January 21 2018).

Gong, X. 2013. Assessment of the Eagle Ford Shale Gas and Oil Resources. Doctor of Philosophy, Texas A&M, College Station, Texas.

Gong, X., Gonzalez, R.A, McVay, D.A. et al. 2014. Bayesian Probabilistic Decline-curve Analysis Quantifies Shale Gas Reserves Uncertainty. *SPE Journal* **19** (06).

Gong, X., Gonzalez, R.A, McVay, D.A. et al. 2011. Bayesian Probabilistic Decline-curve Analysis Quantifies Shale Gas Reserves Uncertainty. Proc., Canadian Unconventional Resources Conference, Calgary, Alberta, Canada.

Gonzalez, R. 2012. Using Decline-curve Analysis, Volumetric Analysis, and Bayesian Methodology to Quantify Uncertainty in Shale Gas Reserve Estimates. Master of Science, Texas A&M University, College Station, Texas.

Gulisano, C.A., Gutierrez Pleimling, A. 1994. Field trip guidebook, Neuquina Basin, Neuquén Province. Proc., IV International Congress on Jurassic Stratigraphy and Geology, Neuquén.

Gutierrez Schmidt, N., Alonso, J., Giusiano, A. et al. 2014. El shale de la formacion Vaca Muerta: integracion de datos y estimacion de recursos de petroleo y gas asociado, provincia de Neuquén. Proc., IX Congreso de Exploracion y Desarrollo de Hidrocarburos Simposio de Recursos No Convencionales: Ampliando el Horizonte Energetico, Mendoza, Argentina, 795-813.

Ilk, D., Rushing, J.A., Perego, A.D. et al. 2008. Exponential vs. Hyperbolic Decline in Tight Gas Sands — Understanding the Origin and Implications for Reserve Estimates Using Arps' Decline-curves. Proc., SPE Annual Technical Conference and Exhibition, Denver, Colorado, USA.

Joshi, K.J. 2012. Comparison of Various Deterministic Forecasting Techniques in Shale Gas Reservoirs with Emphasis on the Duong Method. Masters of Science, Texas A&M, College Station, Texas.

Kanfar, M., Wattenbarger, R. 2012. Comparison of Empirical Decline-curve Methods for Shale Wells. Proc., SPE Canadian Unconventional Resources Conference, Calgary, Alberta.

Lambias, E.J., Laenza, H.A., Carbone, O.. 2007. Evolucion Tectono-magmatica durante el Permico al Jurasico temprano en la cordillera del Viento (3705'S - 3715'S): Nuevas evidencias geologicas y geoquimicas del inicio de la Cuenca Neuquina. *Revista de la Asociacion Geologica Argentina* **62** (2): 217-329.

Legarreta, L., Cruz, C.E., Vergani G. et al. 2012. Cuenca Neuquina. *Buenos Aires*, ed. G. Chebli, J.S. Cortinas, L. Spalletti, L. Legarreta and E.L. Vallejo, 233-250: IAPG.

Legarreta, L., Gulisano, C.A. 1989. Analisis estratigrafico sequencial de la Cuenca Neuquina (Triasico Superior-Terciario Inferior). In *Cuencas Sedimentarias Argentinas*, ed. G. Chebli and L. Spalletti. San Miguel de Tucuman: Correlacion Geologica, Instituto Superior de Correlacion Geologica. Universidad de Tucuman.

Legarreta, L., Villar, H.J. 2011. Geological and Geochemical Keys of the Potential Shale Resources, Argentina Basins. Proc., Unconventional Resources: Basics, Challenges, and Opportunities for New Frontier Plays, Buenos Aires, Argentina.

McVay, D.A., Dossary, M. N. 2014. The Value of Assessing Uncertainty. *SPE Economics & Management* **6** (02): 100-110.

Ministerio de Energia y Mineria de la Republica Argentina. 2016. *Programa De Estímulo a Los Nuevos Proyectos De Gas Natural*, Vol. 74/2016. Boletin Oficial, Gobierno Argnetino (Reprint).

Ministerio de Energia y Mineria de la Republica Argentina. 2017. *Public datasets. Exploration and production data*. Website, Ministerio de Energia y Mineria de la Republica Argentina (Reprint). https://datos.minem.gob.ar/dataset?groups=exploracion-y-produccion-de-hidrocarburos.

Ministerio de Energia y Mineria de la Republica Argentina. 2018. *Public datasets. Exploration and production data*. Website, Ministerio de Energia y Mineria (Reprint). https://datos.minem.gob.ar/dataset?groups=exploracion-y-produccion-de-hidrocarburos.

Morales Velasco, C.A. 2013. Assessment of the Mexican Eagle Ford shale Oil and Gas resources. Masters of Science, Texas A&M University, College Station, TX (August).

Murtha, J. 2006. Some Challenges for Monte Carlo Simulation. *The Way Ahead* **02** (02): 13-18.

Olsen, G.T., Lee W. J., Blasingame, T. 2013. Reserves Overbooking: The Problem We´re Finally Going to Talk About. *SPE Economics & Management* **3** (02): 68-78.

Pourteau, M. 2017. *Programa de Estimulo a las Inversiones en Desarrollos de Produccion de Gas Natural Proveniente de Reservorios no Convencionales - Resolucion 419/17*. Buenos Aires (Reprint). http://argentinambiental.com/legislacion/nacional/resolucion-41917-programa-estimulo-las-inversiones-desarrollos-produccion-gas-natural-proveniente-reservorios-no-convencionales/.

PRMS (Petroleum Resource Management System), SPE/WPC/AAPG/SPEE, November 2011, SPE website www.spe.org/industry/docs/PRMS_Guidelines_Nov2011.pdf

PRMS (Petroleum Resource Management System), SPE/WPC/AAPG/SPEE, August 2018, SPE website https://www.spe.org/en/industry/petroleum-resources-management-system-2018/

Ramos, V.A. 1988. Tectonic of the Late Paleozoic - Early Paleozoic: a colisional history of Southern South America. **11** (3): 168-174.

Sagasti, G., Ortiz, A., Hryb, D. et al. 2014. Understanding Geological Heterogeneity to Customize Field Development: An Example From the Vaca Muerta Unconventional Play, Argentina. Proc., Unconventional Resources Technology Conference, Denver, Colorado.

Sidle, R.E., Lee, W. J. 2010. An Update on the Use of Reservoir Analogs for the Estimation of Oil and Gas Reserves. Proc., SPE Hydrocarbon Economics and Evaluation Symposium, Dallas, Texas.

Stinco, L.P., Mosquera, A. 2003. Estimación del contenido total de carbono orgánico a partir de registros de pozo para las formaciones Vaca Muerta y los Molles, Cuenca Neuquina, Argentina. Proc., II Congreso de HidroCarburos, Buenos Aires, Argentina.

Suarez, M., Pichon, S. 2016. Completion and Well-spacing Optimization for Horizontal Wells in Pad Development In the Vaca Muerta Shale. Proc., SPE Argentina Exploration and Production of Unconventional Resources Symposium, Buenos Aires, Argentina.

Subsecretaria de Energia Mineria e hidrocarburos. 2018. Mapas. Gobierno de la provincia del Neuquén, http://hidrocarburos.energiaNeuquén.gov.ar/?page_id=231 (downloaded January 26 2018).

Uliana, M.A., Biddle, K.T., Cerdan, J. 1989. *Mesozoic extension and the formation of the Argentina Sedimentary Basins*, Vol. 46: Extensional Tectonics and Stratigraphy of the North Atlantic Margins, American Association of Petroleum Geologists (Reprint).

Vaca Muerta Info. 2018. La verdadera Ubicación de Vaca Muerta en el Mapa, http://vacamuertainfo.com/ubicacion-de-vaca-muerta-mapa/ (downloaded January 10 2018).

Valko, P.P., Lee, W. J. 2010. A Better Way to Forecast Production from Unconventional Wells. Proc., SPE Annual Technical Conference and Exhibition, Floerence, Italy.

YPF S.A. 2011. *Actualidad y oportunidades de desarrollo de hidrocarburos no convencionales*. Buenos Aires, Argentina (Reprint).

YPF S.A. 2017. *Investor Presentation*. ypf.com: As of March 2017, YPF S.A. (Reprint). http://www.ypf.com/english/investors/Lists/Presentaciones/YPF-Investor-Presentation-Q1-2017-LTM.pdf.

APPENDIX A

PROBABILISTIC RESERVES ESTIMATES PER WELL

Table 25—Probabilistic oil reserves estimates for individual wells in the BO sub-area

Well number	P90, m^3	P50, m^3	P10, m^3
1	90,678	119,419	160,986
2	48,278	78,678	126,734
3	27,929	46,460	118,854
4	7,250	17,282	63,997
5	12,331	30,575	53,858
6	6,173	16,256	18,193
7	22,281	33,370	64,943
8	495	1,528	12,804
9	66,895	106,234	189,860
10	53,797	65,038	134,974
11	24,741	52,150	105,088
12	3,461	10,711	35,732
13	3,940	4,816	31,542
14	4,155	6,659	23,454
15	47,724	78,854	126,416
16	12,331	40,922	49,102
17	17,792	34,473	111,571
18	15,041	33,254	104,566
19	7,856	15,043	47,144
20	4,252	8,557	41,146
21	24,559	32,150	56,214
22	3,461	10,711	45,732
23	14,044	31,014	54,296
24	9,658	21,390	44,822
25	6,812	9,058	10,741
26	27,226	51,719	137,820
27	45,677	90,040	182,890

Table 26—Probabilistic oil reserves estimates for individual wells in the VO sub-area

Well number	P90, m^3	P50, m^3	P10, m^3
28	72,130	148,447	242,775
29	73,093	188,966	242,123
30	85,275	166,278	357,934
31	49,792	196,346	349,315
32	91,486	128,689	273,980
33	17,169	54,854	195,146
34	11,405	45,364	253,303
35	24,822	105,240	360,317
36	54,330	146,831	377,404
37	81,267	181,493	367,885
38	44,499	182,513	227,804
39	42,650	132,985	215,633
40	166,944	308,416	374,406
41	29,195	124,501	359,250
42	27,610	56,612	283,591
43	55,789	113,885	384,547
44	76,022	109,993	283,785
45	52,045	114,378	375,339
46	87,818	129,673	336,687
47	82,592	109,844	180,025
48	57,631	130,620	351,477
49	107,495	165,122	353,317
50	63,638	120,416	329,063
51	63,278	140,239	384,208
52	100,258	134,936	369,785
53	102,976	141,144	385,078
54	115,101	155,689	323,786
55	127,226	170,233	357,972
56	66,244	95,424	390,245
57	70,998	194,147	397,284
58	73,010	103,874	388,519
59	126,006	177,463	388,093
60	121,662	195,710	389,139
61	45,648	157,071	392,358
62	31,457	216,155	358,366
63	28,962	313,901	368,688
64	121,662	195,710	389,139
65	58,839	249,621	363,023
66	65,964	251,843	390,072
67	111,948	235,724	325,177
68	34,221	76,517	365,798
69	12,317	71,302	152,356
70	31,497	71,790	362,169
71	28,918	65,062	309,843

Table 26 continued

Well number	P90, m^3	P50, m^3	P10, m^3
72	26,299	107,874	345,840
73	43,003	91,593	370,923
74	28,928	76,625	178,541
75	50,758	140,736	358,597
76	83,270	163,225	374,651
77	146,044	227,360	361,737
78	67,062	251,438	374,133
79	77,397	158,213	297,101
80	66,606	112,148	202,672
81	70,132	260,125	391,327
82	84,497	135,337	377,257
83	119,325	287,665	363,186
84	105,890	162,065	378,810
85	40,604	152,256	365,349
86	81,913	214,364	390,378
87	76,457	199,717	383,282
88	51,577	152,760	361,643
89	62,199	171,798	351,289
90	76,685	141,873	367,039
91	110,361	212,927	394,181
92	11,632	46,318	361,752
93	6,522	40,020	377,840
94	65,479	116,384	302,017
95	109,659	187,697	376,201
96	80,264	142,533	352,338
97	59,981	100,070	315,625
98	93,374	199,485	386,176
99	66,748	156,051	354,430
100	114,658	246,068	401,248
101	98,299	238,233	335,218
102	174,404	317,691	364,824
103	88,364	163,270	237,644
104	136,554	212,059	379,883
105	74,136	108,631	177,367
106	33,886	109,218	390,536
107	84,952	176,386	376,402
108	24,779	71,627	376,440
109	80,276	136,876	301,681
110	83,954	132,092	243,027
111	41,790	70,954	295,070
112	78,592	275,574	324,324
113	88,901	153,105	296,834
114	101,576	155,170	389,635
115	16,230	62,151	209,701

Table 26 continued

116	95,006	125,864	225,010
117	69,444	109,112	171,463
118	18,548	71,464	210,508
119	16,562	73,903	206,022
120	89,196	189,011	330,354
121	84,850	133,306	203,735
122	55,652	127,084	379,793
123	46,451	125,635	223,130
124	47,421	117,644	357,219
125	29,316	104,696	320,202
126	29,104	66,297	389,314
127	55,294	135,263	220,284
128	43,006	112,719	375,328
129	63,312	98,333	297,950
130	34,159	104,734	388,872
131	45,771	192,159	360,464

Table 27—Probabilistic oil reserves estimates for individual wells in the WG sub-area

Well number	P90, m^3	P50, m^3	P10, m^3
132	1,323	2,985	6,015
133	16,045	17,198	25,003
134	45,083	71,533	159,879
135	21,659	43,802	139,297
136	5,233	32,124	78,113
137	10,052	29,156	74,918
138	2,195	5,697	12,330
139	18,196	68,114	118,751
140	27,248	67,241	392,652

Table 28—Probabilistic gas reserves estimates for individual wells in the DG sub-area

Well number	P90, m^3	P50, m^3	P10, m^3
141	54,642,924	154,523,528	379,176,740
142	8,920,796	187,990,802	427,852,699

Table 28 continued

Well number	P90, m^3	P50, m^3	P10, m^3
143	5,910,735	93,980,559	334,429,614
144	2,346,259	131,097,878	337,674,934
145	1,971,431	184,061,280	293,538,783
146	74,918,036	153,253,451	399,831,282
147	34,836,507	65,318,028	300,638,953
148	43,189,556	77,099,703	343,592,195
149	27,282,958	57,511,270	397,075,204
150	26,926,833	59,775,461	395,183,456
151	23,175,203	44,062,947	323,425,644
152	10,010,064	17,619,799	313,413,541
153	8,100,867	24,943,934	320,744,275
154	63,027,650	112,800,935	591,629,141
155	11,603,455	54,196,533	291,534,827
156	16,429,314	106,710,206	291,598,841
157	26,843,114	46,797,280	305,737,829
158	9,695,394	21,073,860	454,080,521
159	34,921,907	61,048,227	357,422,948
160	2,061,080	5,334,459	163,141,996
161	2,022,156	3,611,916	160,461,183
162	1,209,174	2,967,738	106,508,894
163	5,449,813	12,495,186	317,398,267
164	5,438,965	23,716,165	362,079,394
165	2,579,777	4,621,077	168,221,237
166	1,959,605	7,051,282	275,609,193
167	936,420	4,013,042	336,588,294
168	8,258,579	23,088,664	317,550,344
169	2,403,984	10,231,054	309,569,649
170	3,871,284	55,348,395	332,132,406
171	1,952,863	5,344,245	231,489,631
172	6,389,925	16,115,800	345,212,978
173	19,826,760	43,688,477	303,845,909
174	4,820,732	11,185,106	307,182,766
175	629,346	1,157,888	99,783,589
176	889,081	3,171,129	239,725,812
177	2,547,452	10,992,696	233,917,029

APPENDIX B

DISTRIBUTIONS AND CORRELATIONS OF DCA PARAMETERS

7.2. BO sub-area: Duong model

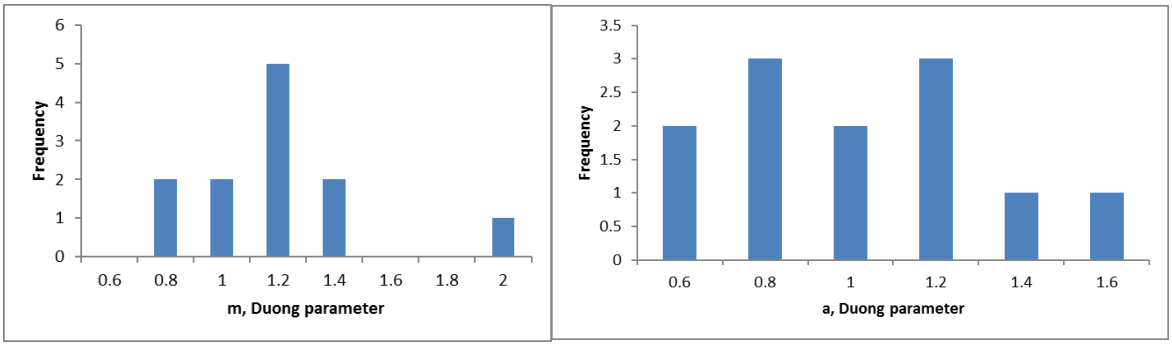

Fig. 22—Histograms of the DCA parameters

Table 29—Correlation coefficients of the DCA parameters

	a	m	Q_i
a	1	0.79	-0.14
m	0.79	1	0.353
Q_i	-0.14	0.353	1

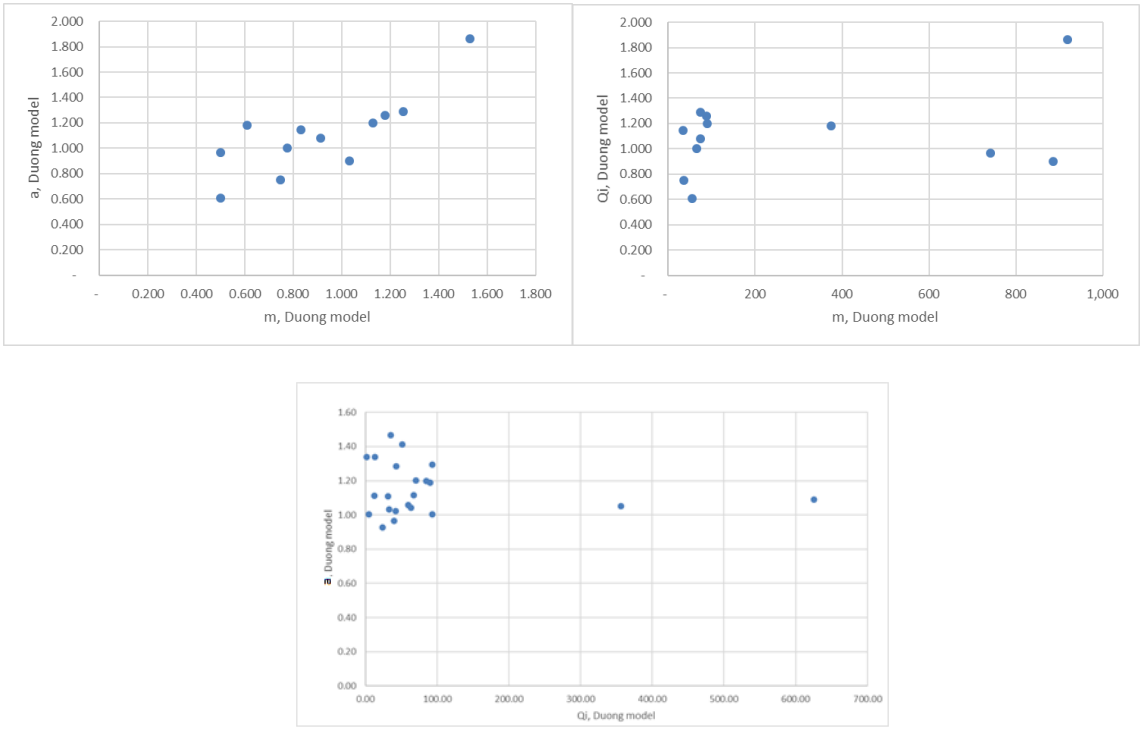

Fig. 23—Correlation plots

7.3. VO sub-area: Duong model

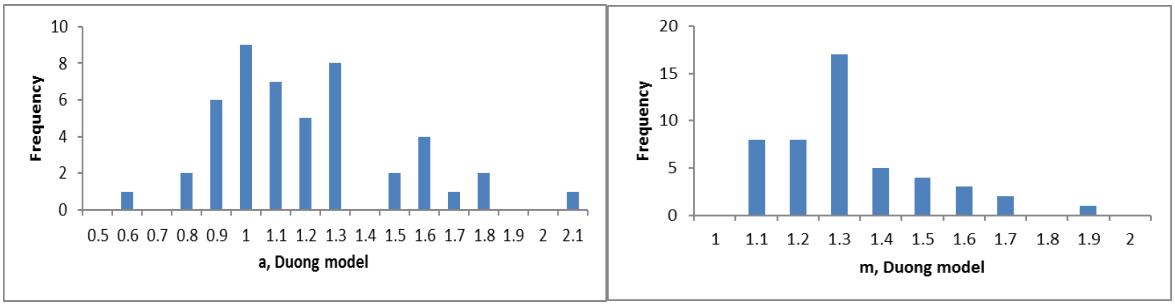

Fig. 24—Histograms of the Duong DCA parameters

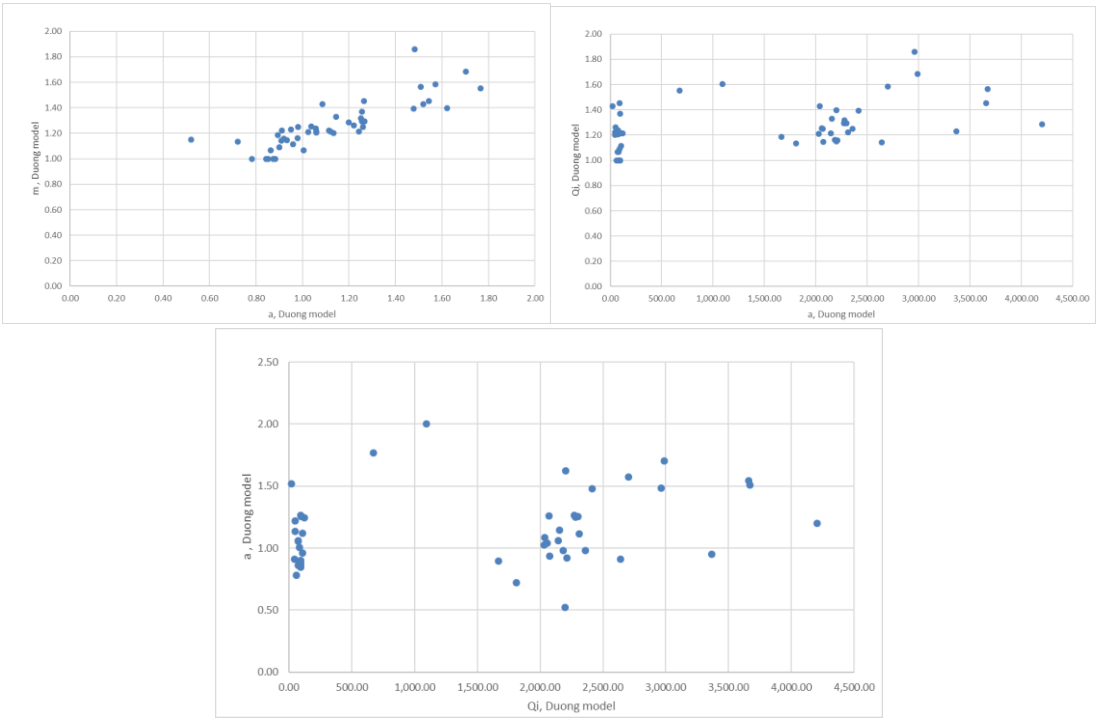

Fig. 25—Correlation plots

Table 30—Correlation coefficients of the DCA parameters

	a	m	Q_i
a	1	0.845	0.256
m	0.845	1	0.446
Q_i	0.256	0.446	1

7.4. WG sub-area: Power Law model

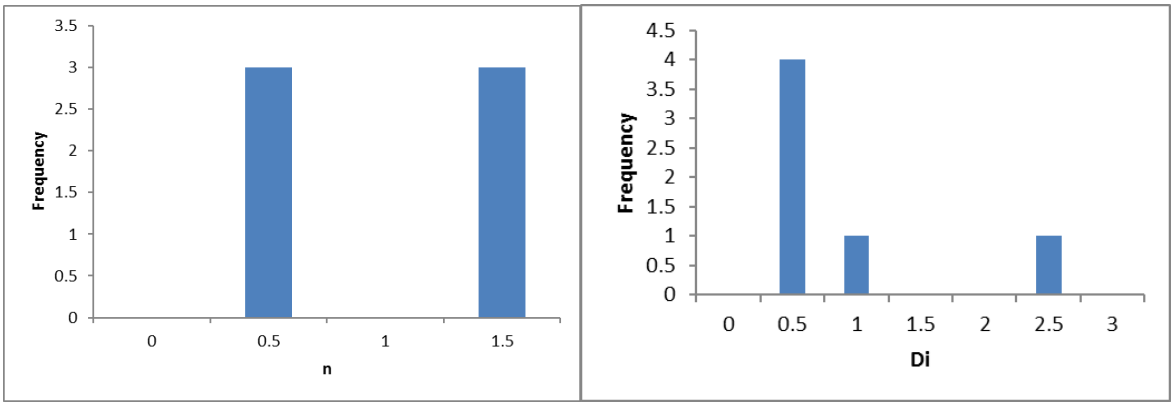

Fig. 26—Histograms of the Power Law DCA parameters

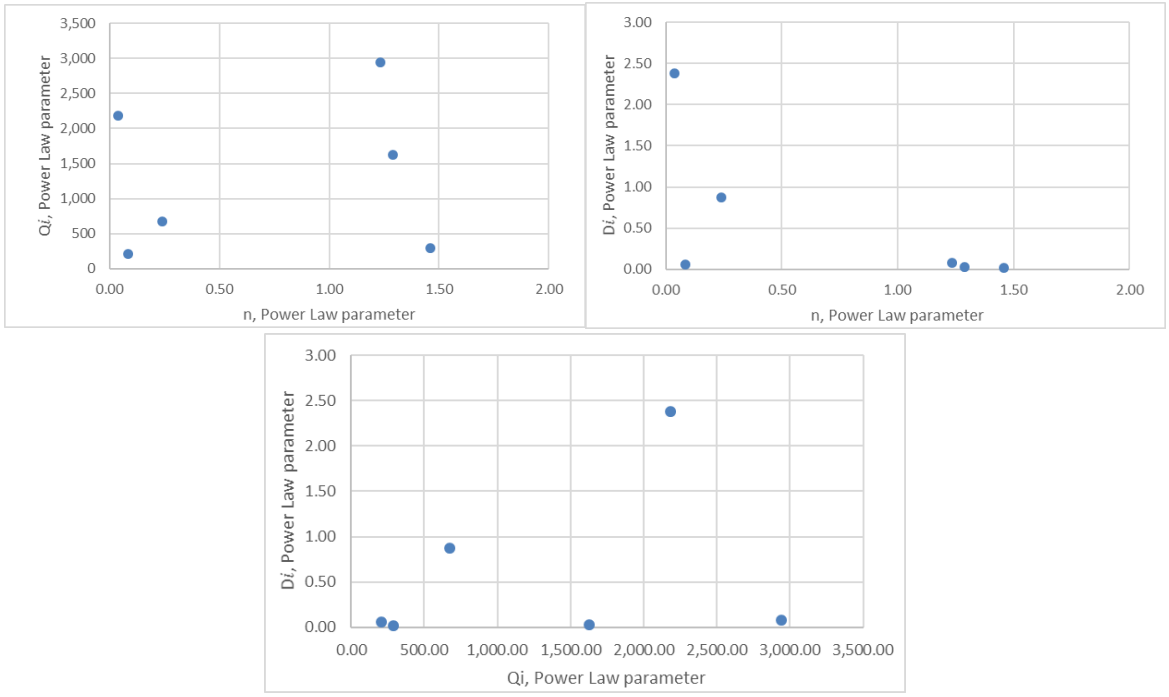

Fig. 27—Correlation plots

Table 31—Correlation coefficients of the DCA parameters

	Di	n	Q_i
Di	1	-0.642	0.292
n	-0.642	1	0.182
Q_i	0.292	0.182	1

7.5. DG sub-area: Duong model

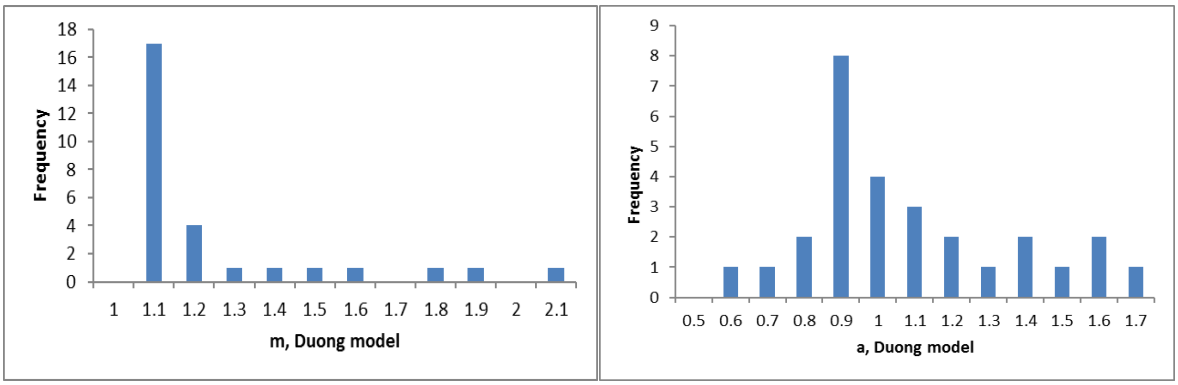

Fig. 28—Histograms of the Duong DCA parameters

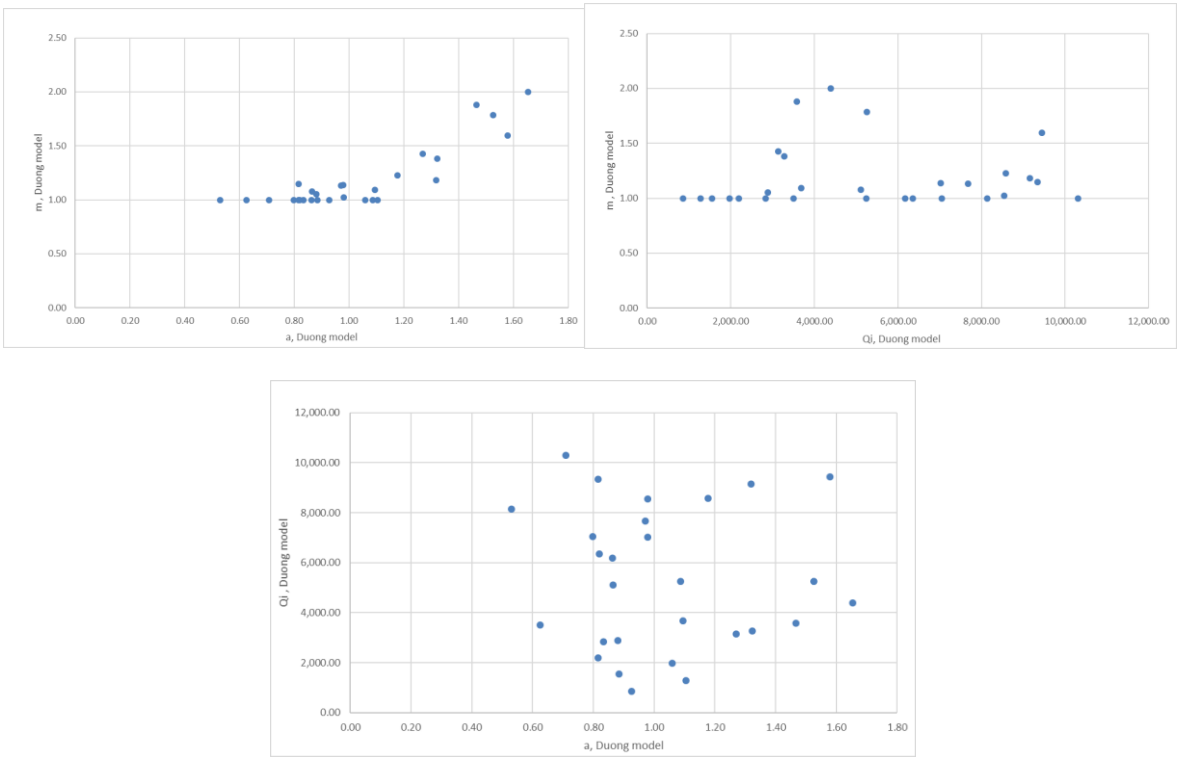

Fig. 29—Correlation plots

Table 32—Correlation coefficients of the DCA parameters

	a	m	Q_i
a	1	0.854	-0.04
m	0.854	1	0.03
Q_i	-0.04	0.03	1